공학석사학위논문

Development of Parallel Genetic Algorithm and Application to Small Modular Fast Reactor Design Optimization

다목적 유전자 연산법을 이용한 소형 조립식 고속로 설계 최적화

2017 년 8 월

서울대학교 대학원

원자로핵공학과

Xiangyi Chen

Development of Parallel Genetic Algorithm and Application to Small Modular Fast Reactor Design Optimization

다목적 유전자 연산법을 이용한 소형 조립식 고속로 설계 최적화

지도 교수 서 균 렬

이 논문을 공학석사 학위논문으로 제출함

2017 년 6 월

서울대학교 대학원

원자로핵공학과

진양의

진양의의 공학석사학위 논문을 인준함

2017 년 7 월

위 원 장 Takuji Oda (인)

부위원장 서 균 렬 (인)

위 원 김 응 수 (인)

ABSTRACT

In multi-objective nuclear reactor design problem, instead of implementing a single-objective optimization "scalarized" from the multi-objective problem, for example, by assigning each objective an importance, it is beneficial to provide a trade-off-surface to the decision maker for further consideration. However, the relatively expensive calculation in the nuclear reactor design prevents the true Pareto front to be established. Instead, the "pseudo-trade-off surface" is usually provided. Thus, when a preferred solution has been decided, the decision maker comes to face the question that whether this solution is the non-dominated solution. The Genetic Algorithm with the "valuable phenotype" archival rule developed in this work abnegates the logic that higher quality individuals should have the priority to be selected. The new rule addresses more about of the balanced accomplishment of the objectives rather than pitch into the elitism. This Optimized Logic Genetic Algorithm has demonstrated its efficiency and robustness in assisting the designer to obtain the better flexibility by providing the diverse potential solutions that can dominate or are similar to the interested solution on the "pseudo-trade-off surface".

Keywords: Genetic Algorithm, Multiobjective Optimization, Nondominated Sorting, Valuable Phenotype, Small Modular Fast Reactor

Student Number: 2015-22151

CONTENTS

LIST OF TABLES

LIST OF FIGURES

1. Introduction

1.1. Background

In 1895, Charles Darwin in his book “On the Origin of Species” proposed the hypothesis of Evolution, which kicked start the evolutionary biology. In this hypothesis, random variations of natural selection happening to a large size of population during numbers of generations is the mechanism of what shapes the creatures today. From the point of view of this hypothesis, if we can conclude that the creatures today fit the nature in a higher tier than the past, the evolutionary method is naturally a kind of solution-oriented method. Inspired by this hypothesis, evolutionary computation was born that can be traced back to 1950s after the invention of the first computer (D. Dasgupta, 1997) and then undergoes the rapid expansion. It now becomes a branch of algorithms for global optimization in computer science. The Genetic algorithm (GA), a class of evolutionary method, since it was taking off in 1975 especially after the 1990s when the computers are easily accessible has been presenting itself in a wide range of applications covering optimization, automatic programming, signal processing, bioinformatics, social systems (Jong, 2005). In nuclear reactor design arena, numerous publications have demonstrated the strength of GA because of its consistent parallelizability and multi-objective feasibility which suit the high complex nuclear systems optimization. Benefit from its efficiency, the GA has successfully applied in the designing of various types of reactors like pressurized water reactor, pressurized heavy water

reactor, boiling water reactor, advanced gas cooled reactor, research reactor, fast reactor, and with a broad range of problems including the loading pattern, the burnable poisons, the core design, and the online refueling (Jayalal, Murty, & Baba, 2014). Recently, with the growth of computational capacity, the study in this area has put its finger on system level optimization problems with neutronics and thermal-hydaulics coupling (Kumar & Tsvetkov, 2015a)(Kumar & Tsvetkov, 2015b). Motivated by the new progress, in this work, an Optimized Logic Genetic Algorithm (OLGA) is proposed which can increase the flexibility for the designer to find a better solution in nuclear reactor design and it is applied in a small modular fast reactor optimization.

1.2. Objective of the Study

It has been widely recognized that when a designer is facing a multi-objective optimization problem to search out the dominant solution that can overwhelm all other solutions in all of the objectives is almost impossible for the inherent confliction between one objective and the other(Toshinsky, Sekimoto, & Toshinsky, 2000). Instead of having a preconception of the importance of each objective, usually, a trade-off surface is provided for further consideration. A typical trade-off surface (Pareto front) gives a dozen or more solutions with the performance values of objectives that each solution on the trade-off surface does not dominate and cannot be dominated by other solutions. There are myriad methods have been developed to detect and form the trade-off surface in Genetic Algorithm, however, during the optimization process, whether all the points on the trade-off surface have arrived the

exact front position that cannot be dominated is still a question. In nuclear design, it is even harder to arrive the true Pareto front because of the expensive computation. Thus, what actually obtained in practice is a "pseudo-trade-off surface" that is formed by pseudo-local-optima as shown in figure 1-1. Based on the values of the objectives in the aid of the knowledge from the designer, a preferred solution on the pseudo-trade-off surface can be determined. However, this should not be marked as the end of the optimization because of the solution is probably not on the true Pareto front. Thus, it is of significance to start from this point and detect the potential solution that can dominate this preferred solution. In this work, the OLGA is developed with the objective to serve the role to search the potential solutions that are in the higher tier than the preferred solution and provide the decision maker diverse options.

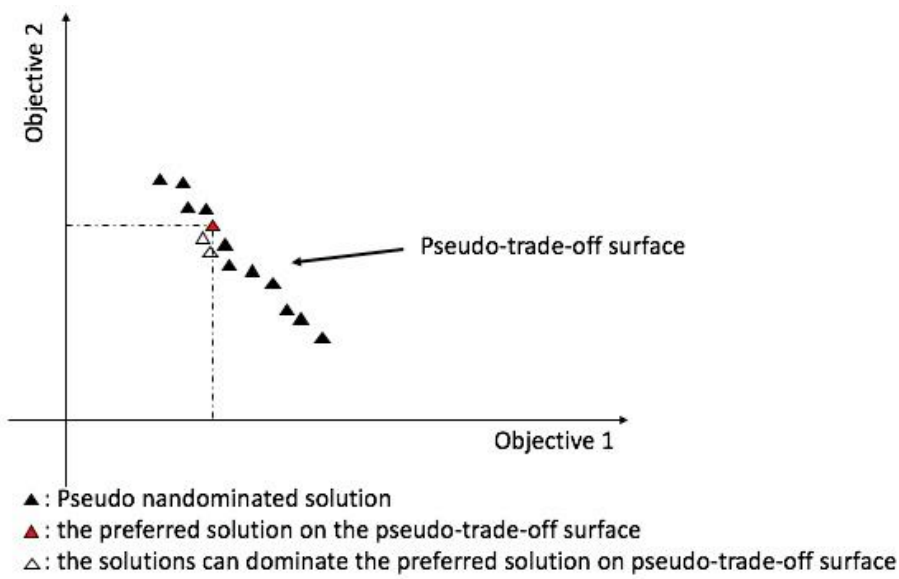

Figure 1-1 One example of Pseudo-trade-off surface in the optimization to minimize Objective 1 value and Objective 2 value

1.3. Reference Reactor and the Interested Pseudo-Local-Optimum

The reference reactor taken in this study is a Lead Fast Reactor - Battery Omnibus Reactor Integral System (BORIS) developed in NuIDEA at Seoul National University (Hyung Min Son & Suh, 2011). The concept of BORIS is based on the envision that in the developing communities, particularly in the remote islands can be supplied with electricity generated by a safe, reliable, economic and sustainable Generation IV nuclear system (GIF, 2014). One design from previous optimization work is taken as the pseudo-local-optimum given in table 1-1 and the sketch of BORIS is shown in figure 1-2 (Son and Suh, 2014). The thermal power of BORIS is 22.2 MW, which can last for more than 20 years without refueling. The 0.8-meter-high reactor active core is fueled with nitride natural uranium and Pu and Minor Actinides extracted from spent fuel. The heat exchanger is selected as an once-through type with primary coolant flowing down in shell side and secondary working fluid S-CO_2 flowing upward in tube side. Totally six heat exchangers are bounded inside the reactor vessel at the upper berth of the downcomer. The coolant flow area in heat exchangers is designed the same as the channel connecting upper plenum and heat exchanger. In the core, hexagonal fuel rod lattice is adopted and the core is installed with 757 fuel rods and five grid spacers.

The materials selected for fuel, primary coolant, reflectors, cladding are shown in table 1-2 (Hyung M. Son & Suh, 2014). The Pu-MA extracted from a conventional Pressurized Water Reactor are shown in table 1-3 (Buongiomo, 2001). The ferritic–martensitic HT9 is chosen as cladding material and axial reflector which has been

widely studied in sodium fast reactor and lead fast reactor (Pahl, Porter, Lahm, & Hofman, 1990)(Pahl, Lahm, & Hayes, 1993)(Allen & Crawford, 2007)(Sobolev, Malambu, & Abderrahim, 2009). The radial reflector and reactor vessel material are SS316 in current design.

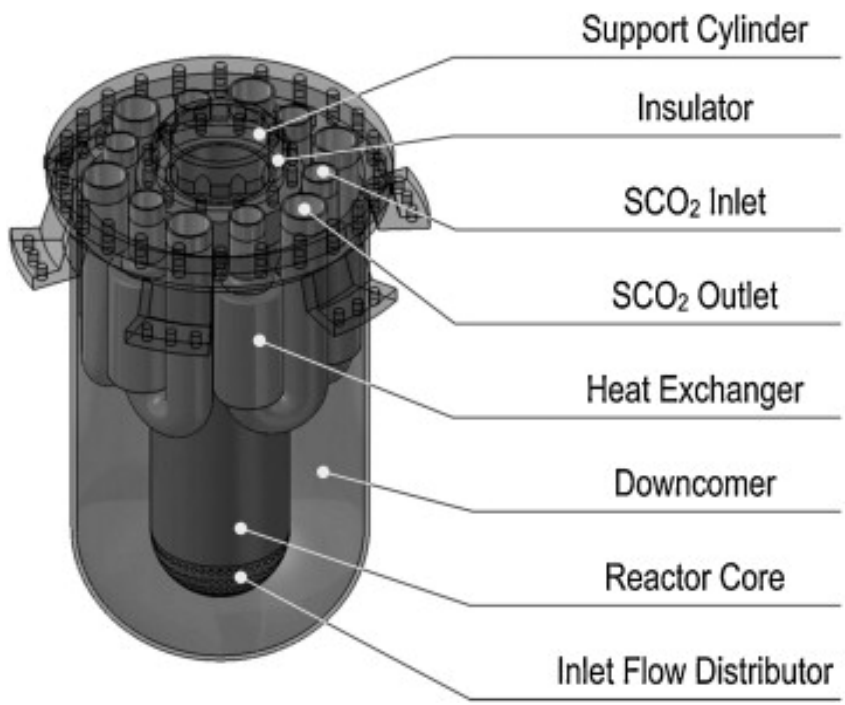

Figure 1-2 BORIS reactor assembly (Son and Suh, 2014)

Table 1-1 One pesudo-local-optimum design of BORIS

Parameters	Values
Thermal Power [MW]	22.2
Pu-MA Fraction	0.20
Core Diameter [m]	0.9828
Fuel Pellet Diameter [m]	0.02363
Active Core Height [m]	0.8
Pitch-to-Diameter Ratio	1.1
Fuel Pin Diameter [m]	0.028
Cladding Thickness [m]	0.001
Riser Length [m]	1.9
Riser length + Active Core Height + Upper Plenum Length [m]	4.3
Core Inlet Temperature [K]	713.15
Outlet Temperature [K]	831.0
Primary Mass Flow Rate [kg/s]	1298.5
Number of Heat Exchanger	6
Number of Tubes/Unit	1200
Heat Exchanger Tube length [m]	1.0
Heat Exchanger Tube Outer/Inner Diameter [m]	0.016/0.012
Heat Exchanger Pitch-to-Diameter Ratio	1.2

Table 1-2 Materials used in BORIS

Materials	Value/Parameters	Description
Fuel	U-Pu-MA nitride fuel	N-15 is used
Primary coolant	Pb/Pb-Bi	-
Cladding	HT9	-
Axial reflector	HT9	-
Radial reflector	SS316	-

Table 1-3 Higher actinides from LWR spent fuel (Buongiomo, 2001)

Isotope	**Weight percent**
Pu composition	**100% =80% total**
Pu238	2%
Pu239	58%
Pu240	26%
Pu241	10%
Pu242	4%
MA composition	**100% = 20% total**
Np237	43%
Am241	45%
Am242	0%
Am243	9%
Cm244	3%

1.4. Optimization Problem Description

To achieve long-life once-through operation, the BORIS uses U-Pu-MA-N as fuel in the reactor core in which the natural Uranium serves as the fertile material and the Pu-MA extracted from spent fuel from PWR acts as the fissile material that is burnt to keep the reactor above criticality. It is notable that when Pu-MA fraction is large, the excessive reactivity at the Beginning of Life (BOL) is much larger than what it is in lower Pu-MA fraction fuel and this is not desirable because of the increasing reactor complexity with the increasing number of control rods; eventually there will be more risks of the control rods malfunction (Todreas, 2001). Thus, the fraction of Pu-MA or the fraction of natural uranium in the fuel recipe should be picked out carefully to assure the criticality in successive 20 years and achieve the low BOL reactivity which becomes the first objective. Another consideration of neutronics design is related to the MA destruction. According to the study of Choi et al. and Todreas, a harder neutron spectrum is especially beneficial for increasing the

total MA depletion rate (H. Choi & Downar, 1999) (Todreas, 2001). In this work, the higher fast neutron flux ratio which is indexed by the fraction of neutron flux with the energy above 0.1 MeV and the higher value of this index becomes the second objective. The elevation difference between the hot center and the cold center is an important parameter that can affect the driving force for natural circulation. A well-designed height of the reactor can not only provide sufficient drive force but also shape the reactor more compact. In this study, the height summation of the active core, the upper plenum and the riser are chosen to index the compactness while the reactor core diameter is kept constant which will guarantee radial configurations in previous design will not be changed. Therefore, the lower height becomes the third objective. In the economic consideration, a higher primary side outlet temperature can increase the thermal efficiency of the secondary system(Qualls et al., 2017)(Ahn et al., 2015). Thus, it becomes the forth objective. For the integrity of the fuel rods consideration, the maximum cladding temperature, the maximum fuel center temperature and the maximum velocity in fuel bundles are chosen as the constrains with the upper limit values as 923.5 K, 1673 K and 2 m/s(Cheon et al., 2009)(Smith, Kim, Bodnar, & Wade, 2005)(Hyung M. Son & Suh, 2014).

In this work, to limit the computational complexity, the fuel rods position, the fuel bonding gap, the thickness of the cladding and the fuel volume in this reactor is kept constant as shown in figure 1-3. Thus, the fuel rods pitch is constant while the Pitch-to-diameter ratio is adjusted by the different fuel pellet diameter. The Pitch-to-diameter ratio will affect the thermal-hydraulic performance of the reactor as well as the neutronics performance. A loose fuel rod bundles configuration will enhance

neutron moderation so that induce a lower fast flux ratio, however, it is meritorious for decreasing the hydraulic resistance and strengthening the heat transfer concurrently. Meanwhile, the active core height and upper plenum are also dependent on the fuel pellet diameter which will affect the hot center and cold center elevation. Thereby, the reactor core inlet temperature and riser height are adopted to achieve the thermal efficiency, compactness objectives and meet the constraints of the integrity of the fuel rods. The input parameters, the objectives and the constraints are summarized in table 1-4.

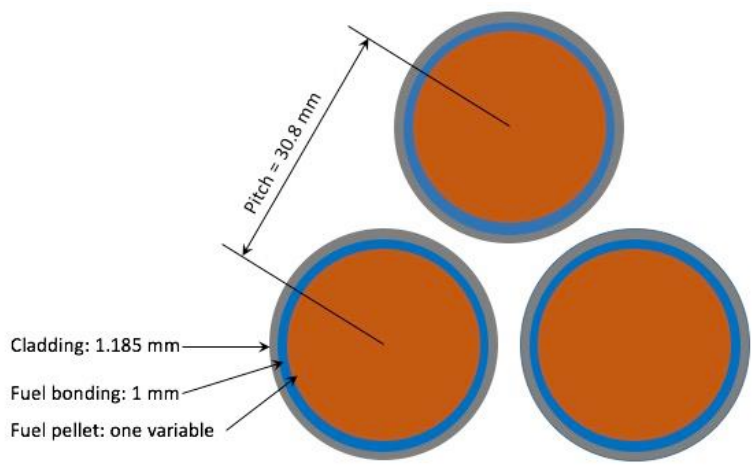

Figure 1-3 Fuel pins configuration

Table 1-4 Input parameters, objectives and constraints

Parameters	Inputs/Objective/ Constraint Indexes	Objective/limitation
Fuel Pellet Diameter [cm]	Inp1	1.8-2.6 (precision: 0.001)
Fissile Material Fraction	Inp2	0.2-0.27 (precision: 0.0001)
Core Inlet Temperature [K]	Inp3	650-790 (precision: 0.1)
Length of Riser [m]	Inp4	0.0-2.46 (precision: 0.01)
BOL Effective Criticality	Obj1	Lower than the pseudo-local-optimum
Fast Neutron Flux Ratio	Obj2	Higher than the pseudo-local-optimum
Primary Side Outlet Temperature	Obj3	Higher than the pseudo-local-optimum
Reactor Height (active core + upper plenum + riser length)	Obj4	Lower than the pseudo-local-optimum
Maximum Fuel Temperature	Cstr1	Upper limit 1673 K
Maximum Cladding Temperature	Cstr2	Upper limit 923.5 K
Maximum Coolant Velocity	Cstr3	Upper limit 2 m/s

2. Genetic Algorithm and the Operators

2.1. The Simple Genetic Algorithm

Similar to other evolutionary methods, GA works within the scheme of the adaptive heuristic algorithm. It mimics the hypothesis of the creatures evolution in the way of competition, selection and heredity proposed by Charles Darwin. In scientific computation field, Holland is recognized as the first one rigorously

proposed the theory of Genetic Algorithm (Holland, 1975). In his proposal, the evolution of populations is simulated in generation series. During the evolution, each individual in the population carries a unique chromosome that represents the parameters need to be optimized. The quality of the parameters reflected by the behavior of the system are synthetically evaluated by the fitness function. Based on the fitness evaluated, the elitists are selected to produce offspring, and the poor-quality individuals are dumped. The working process of GA is illustrated in figure 2-1. The process starts from generating a random population with certain size; then the population enters an iteration loop. At the beginning of this iteration loop, the population is evaluated by the fitness function, and these individuals in the population are marked with a fitness value. The individuals will then be judged by their fitness value which will determine the probability that they are can survive in the selection process to produce offspring. During the offspring production process, some portions of chromosomes from the father and mother undergo a crossover to form the initial chromosome of the children and the mutation takes place forthwith. As times goes on, it is hoped that the system will behave better in average as well as in the elitists in later generations. In this section, the encoding methods and the necessary operators frequently used in GAs are introduced, and some innovative methods and operators are reviewed.

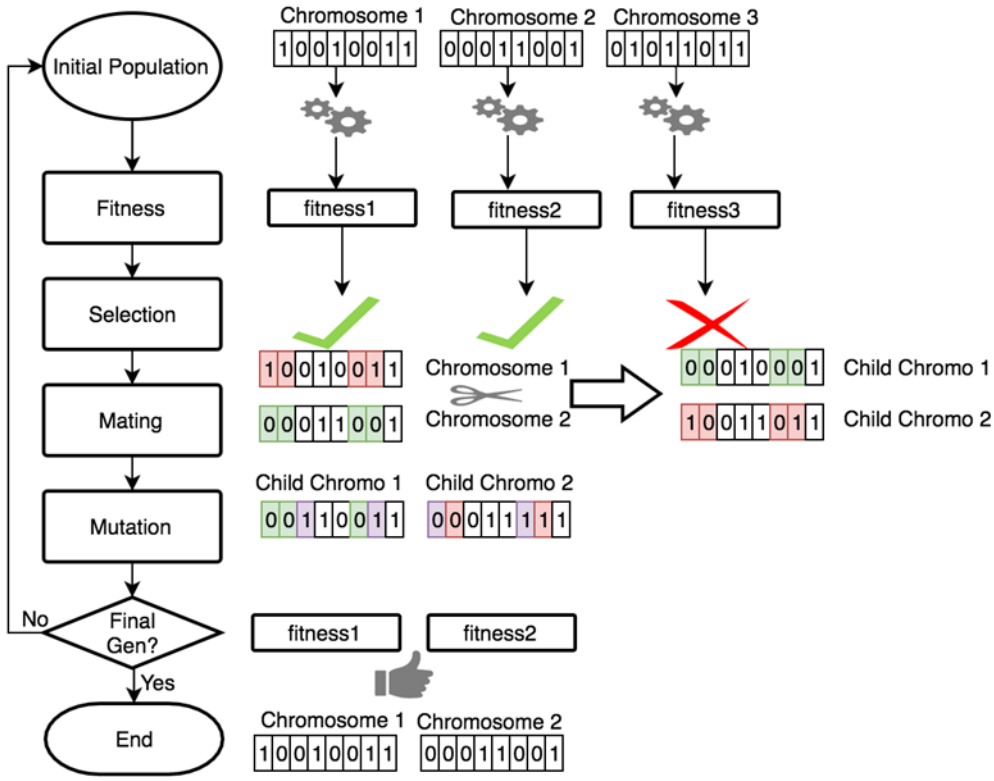

Figure 2-1 A simple Genetic Algorithm

2.2. Chromosome Encoding Method

Encoding, by definition, is simply transfer the information in one form to another for efficient transmission, operation and storage. In different application, the different encoding method can be used. Thus, immeasurable encoding methods have been developed in GAs.

The most commonly used encoding method is Binary Encoding. For example, there are 2 variables need to be optimized. Each one has a range from 0 to 100 with the precision of 1. Then they can be written in binary expression from 0000000 to 1100100. In programming code, the pair of parameters like (12,69) in the first

individual and (59,98) in the second individual are then encoded as 00011001000101 and 01110111100010 in which the first seven digits represent the first variable while the last seven digits represent the second variable. The benefit of using binary encoding method is that it can be easily operated in crossover to change two variables at the same time if the portion selected to crossover crosses the joint of two variable sections e.g. from the sixth digits to eighth digits are selected in crossover operation. This cross-variables crossover effect can induce the slow convergence but the higher efficiency in the exploration of the search space.

Another encoding method called Real-Valued Encoding can be used more straightforward. For instance, if the search domain consists eight dimensions, each one has a range from 0 to 100. Then, a possible code used in a program can be (23, 43, 11, 57, 99, 67, 43, 54) in the list format. In some tasks, the permutation encoding is more suitable. Take the fuel loading pattern problem as an example, if we have totally 9 fuel assemblies with different enrichment in a research reactor, then a possible pattern can be (9, 3, 5, 7, 2, 8, 1, 6, 4), while another possible pattern can be (2, 1, 9, 6, 8, 4, 5, 7, 3). Except for the most frequently used chromosome encoding method introduced above, under some circumstances, customized encoding method like trees, matrix encodings, structured heterogeneous encodings can be employed for the convenience of the targeted problems (D. Dasgupta, 1997).

2.3. Selection Operator

Comparing to the encoding method, selection method plays a more significant role in GAs and has attracted more studies. Based on the elitism according to

evolution hypothesis, the genes of fittest ones should be handed down to the succeeding generation. So, most of the selection are following this idea. In the next paragraphs, the commonly used selection methods are introduced, and some innovative selection methods are surveyed.

The Roulette Wheel Selection is widely used in the cases when the fitness of the individuals at different level do not vary widely. In this method, the parents are selected by the possibility based on the weight fraction of their fitness values from overall fitness value. The reason it is applicable only to narrow range of the fitness is that when very few like one or two individuals consists the dominant weight of the overall fitness, the offspring can highly depend on the genes from these individuals and consequently the evolution losses its diversity in exploration of the search space. There is one way called Rank Selection can treat this problem of Roulette Wheel Selection. When every individual is ranked by its fitness, the absolute dominance effect disappears in the sense of rank numbers, then the Roulette Wheel Selection can be safely applied using rank numbers instead of fitness values.

Elitism Selection is the most candid and powerful method; it promises a rapid convergence. In this method, the best a few individuals with best fitness are preserved to next generation, while other individuals are selected in other convectional ways like the Roulette wheel and Rank selection. This method inhibits the operation of crossover and mutation to destroy the elitists, so the fitness of elitists never declines but the problem is the diversity may be cracked. The Tournament selection considers the potential of poor quality individuals while keeping the priority of the high-quality individuals. In the Tournament, two individuals are

chosen randomly at the same time, and the one with higher fitness will be selected.

In order to increase the optimality of the solution, innovative selection methods are designed for special cases. Correlative Tournament Selection (CTS) and Correlative Family-based Selection (CFS)(Matsui, 1999) proposed by K. Matsui is derived from the thought that there is a correlation between individuals that once mated will have a higher possibility to produce children similar to them. The similarity correlation can be formed from Hamming distance which measures the minimum number of bits need to be changed from one string to the other. So, once the parents are kept in large Hamming distance, the diversity will be preserved. The CTS and CFS are tested in the Royalroad and the Non-Stationary Knapsack Problems. They are found to be superior to conventional selection methods.

Instead of always keeping the parents with high discrepancy to mate, Marcus invented the Fitness Uniform Selection Strategy (FUSS)(Hutter, 2002) based on the fact that individuals tend to attach itself to local optimum once the "local optimum trap" emerged. This tendency may hurt the diversity as time passing. So, the selection pressure should be adjusted to be lower value to keep the diversity as the average fitness increasing. In FUSS, the individuals are steady created from every fitness levels to insure the selection pressure is burdened by all groups. This method is compared with the standard selection (STD) in a simple 2D example. It shows to be much more effective than STD.

The Cluster Selection Method (CSM) (Alkhayri, 2016) is invented recently and compared with STD in the famous Traveling Salesman Problem (TSP) which requires one to find the optimal path when a salesman is traveling between a set of

cities(Laporte, 1992). The CSM divides the population into clusters by the similarity of their fitness. In each cluster, the cluster value is estimated to represent the quality of individuals inside. The selection is processed inside each cluster and the number of individuals to be chosen is based on the cluster value. The result shows its prevailing efficiency in this problem.

2.4. Crossover Operator

The essence of GAs is the Crossover Operator. The selection method is used to preserve the perfect characteristics of elitists, but the crossover is the powerful tool to create even high-level elitists. The following paragraphs will introduce the conventional crossover method as well as some new conceptions in the crossover method.

The crossover can be happening in single piece or multi-pieces in chromosomes; usually the cutting points are chosen randomly in the chromosome. In binary encoding, the two chromosomes from the mother and the father can be cut by a single point, and one portion of the chromosomes are exchanged which can produce two children. Multi-point crossover will cut the chromosomes in two or more points and the portions of the chromosomes are exchanged dispersedly. According to the study of Wu and Chow, multi-point crossover present better performance than single point (Wu & Chow, 1995). Another way of the crossover operation is randomly choosing the bits to exchange which is called Uniform Crossover. The Real Value Encoding shares the same crossover method as the Binary Encoding. However, there is the natural difficulty in the crossover operation in Permutation Encodings that the

crossover method introduced above can cause repeated values which is inhibited. For example, if the father chromosome is (1,2,3,4) while the mother chromosome is (2,3,4,1), apply one-point crossover in the middle of the list, then the children chromosomes become (1, 2, 4, 1) and (2, 3, 3, 4). That means the ordering encoding crashes in some items while some other items disappear. There are various ways to fix this problem. The simplest thinking is to do the point crossover as it is, then implement some modification on the second portion of the children's chromosomes. The modification can be deleting the digits repeated and create the digits disappeared by certain rules. Apparently, the drawback exists that the method induces partially loss of the characteristics of the parents. To settle this problem, P. E. Poon proposed a universal crossover operator for ordering applications called Tie-Breaking Crossover (TBX) (Poon & Carter, 1995). The TBX preserves the point cross-over in the conventional manner and then generate a random array from 0 to the dimension of the order list minus 1 e.g. (0, 1, 3, 2). Then do the multiplication of the children chromosomes with the dimension of the order list, then (4, 8, 16, 4) and (8, 12, 12, 16) are produced. By taking the summation of the new children chromosomes and the random array, the crossover map is formed as (4, 9, 19, 6) and (8, 13, 15, 18). Finally, the ultimate children's chromosome order is determined by the order of the crossover map that the produced chromosomes become (1, 3, 4, 2) and (1, 2, 3, 4). Though this is a clever way to make the game fair but it does not emerge to be more efficient when comparing with the previous permutation crossover method (Poon & Carter, 1995).

Since the crossover operator is assumed to preserve excellent characteristics

from the parents, some new designs are initiated for pursuing enhancement of this effect.

The first thinking is whether it will work better when various crossover methods work together. In the work of Mustafa Kaya, the One-point crossover, Multi-point Crossover, Variable-to-Variable Crossover, Uniform Crossover and Mixed Crossover and Direct Design Variable Exchange Crossover are randomly chosen in the crossover operation (Kaya, 2011). This idea is tested in the Reinforced Concrete Beam Problem, but the feedback shows the obtained fitness value are no better than other mono-crossover methods.

The selection of crossover points is another issue; the random choosing crossover points raises the concern from Mengjie Zhang etc. for it can destroy the good "building blocks" which is a portion of chromosome keeps good quality of the individual (M. Zhang, Gao, & Lou, 2007). Thus, a Looseness-Controlled Crossover (LCC) is introduced. In this method, if a child has better fitness than its parents, the crossover is treated as successful one, the crossover point is recorded, then the blocks between these crossover points are called good building blocks and all the good building blocks are combined to form a bigger building blocks. When the iteration goes on, the good building blocks grow up. In order to avert disruption of the good blocks, LCC will only link the identified individuals containing the similar good blocks together to mate. This method is tested in three different image data sets experiment; the results prove that it is much more efficient than the standard crossover operator in this task.

Another study also seeks to revise the arbitrariness of crossover points. Kusum

Deep et al. proposed the Laplace Crossover operator (LX) (Deep & Thakur, 2007). The LX adopts Laplace distribution to determine the distance between points. This invention is compared with 20 benchmark problems and shows outperformance.

2.5. Mutation Operator

Selection and Crossover both take the advantage of the elitists in the aspect of surviving ratio and gene inheritance which are vigorous methods to produce better offspring. However, both of them induce the tendency to a local optimum. The mutation operation works like a brute-force engine to save the evolution from the predicament. The mechanism of mutation is to change the value in some portions in the encoded string, which is expected to be capable of exploring the untouched area. The following paragraphs are going to introduce the conventional mutation operators and some novel proposals.

The mutation operation is also an encoding method dependent operation. In binary and real value encoding, it randomly selects the one or more points to mutate. If the target position is 0 in binary string, then it flips to be 1 while if it is 1 then 0 is placed. In real value mutation, the mutated value can be any number in the range of the search space. However, in the permutation encoding, more than one point should be identified and then their positions are exchanged. Though mutation operation will expand the searched area, it should be managed gingerly. Because mutation may cause the large-scale destruction of promising offspring and further induce the evolution to be entirely random. In the study of Randy L. Haupt, it is suggested that the probability of mutation should be in the range of 0.05 to 0.35 (Haupt & Haupt,

2000).

In mutation methods study, considerable efforts have been put to avoid the collapse of the evolutionary progress while keep greater searching ability. Doo-Hyun Choi proposed Accelerated Evolutionary Programming (AEP) which is a back-propagation learning algorithm. In AEP, the mutation rule is adjusted by neural network learning from the experience of previous generations. By using the benchmark test functions, results present the charming characteristics of AEP that the evolution using the back propagation mutation rule converged to global optimum more faster (D. H. Choi & Oh, 2000). In the work of Qingfu Zhang et al., an "Evolutionary Algorithm with Guided mutation" (EA/G) is adopted in solving the Maximum Clique Problem. In this method, the exploration is conducted in different subspaces in various generations. The mutation operation is a function of the parents, probability vector and the mutation probability. The probability vector is created by PBIL algorithm which reflects the distribution of promising solutions global wise. By combining the global information of probability vector and location information of the parents with mutation probability, the offspring can have better quality than conventional static mutation possibility method (Q. Zhang, Sun, & Tsang, 2005).

3. Optimized Logic Genetic Algorithm

3.1. Non-dominated Sorting Genetic Algorithm with Valuable Phenotype Archive

In the non-dominated Sorting Genetic algorithm, instead of implementing a single-objective optimization "scalarized" from the multi-objective problem, for example, by assigning each objective an importance, it is a posteriori method that usually provide a representative subset of Pareto optimal solutions. Employed with sharing function and niche count technique, the Non-Dominated Sorting Genetic Algorithm (Srinivas & Deb, 1994) and Non-Dominated Sorting Genetic Algorithm-II (NSGA-II) (Deb, Pratap, Agarwal, & Meyarivan, 2002) are the most famous methods in this kind. Both of these two algorithms are evolved from the idea of nondominated sorting procedure which was proposed by Goldberg (Goldberg, 1989). Parks also borrowed the idea and created the non-dominated sorting genetic algorithm with archive which uses the archived elitist population to boost the formation of the frontier (Parks, 1996). Inheriting from the Parks' method, Toshinsky et al. improved the rules of archive which shows that the solutions are more close to the optima (Toshinsky et al., 2000). The archival rules used in the work of Toshinsky etc. are (Toshinsky et al., 2000):

1, if the new solution dominates any members of the archive, those are removed, and the new solution is added;

2, if new solution dominated by any members of the archive, it is not archived;

3, if new solution neither dominates nor is dominated by any members of the

archive, it is archived.

Besides using the archive to generate the offspring, a Set of Potential Parents (SPP) is used to store the dominated population to generate the same number of child chromosomes as those generated by the archive (Toshinsky et al., 2000).

While this method is prevailing in finding the pseudo-Pareto-front, the merit is not rewarded when the problem is to exploit around one pseudo-local-optimum which is different from pushing the Pseudo-front forward. Specifically, since the pseudo-local-optimum is one of the point on the pseudo-Pareto-front which can be thought as a biased solution with a determined weightiness for each objective, in many objective optimization, the potential of some objectives has more likely been exhausted than others that the performance in these exhausted objectives are significantly tougher to be improved. Alternatively stated, during searching a solution that can dominate the chosen solution, the performances of one or more objectives pretend to be degraded while the others pretend to be improved. For this reason, the previous rules are elaborated, and the significance of the accomplishment of the tough-objective(s) is addressed, and in this way, it is expected that the accomplishment of objectives will be more balanced, eventually, the higher tier of solutions than the pseudo-local-optimum can be searched out efficiently and robustly. Based on this idea, the rules of archive in the methods used by Parks and Toshinsky et al. are modified as shown in figure 3-1. The main difference is that the solution with “valuable phenotype” is well appreciated. The individual with “valuable phenotype” means the individual has met the tough objective. In the process of searching, the archive is tallying the total number of the accomplishment of each

objective in the archived member and decide which phenotype is valuable, thus as the generation goes on, the accomplishments of the objectives are equally carried out by the archived members.

Since, the purpose is to find the solutions that can dominate the chosen solution instead of pushing the entire frontier forward, the rank is determined by the number of the objectives accomplished. Thus, the higher rank means a better quality of this solution. This is reasonable that pushing the values of certain objectives further than others means the searching is more biased to the neighbor local-optimum and it is harder to find the solutions can dominate this chosen solution. Instead of distinguishing the quality of solutions by the performance it has improved in each objective during the process, the best quality solutions can be revealed after they are washed at the end of searching.

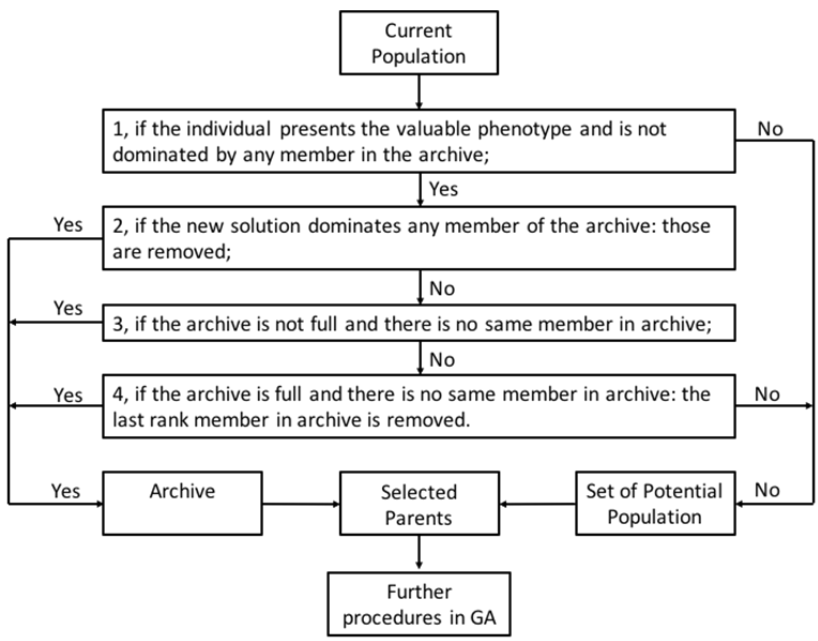

Figure 3-1 The proposed rule of archive

3.2. Development of Parallel Computing Framework

The framework of optimization is developed using Python programming language for its portability in various operating systems and prominent interfaces to other programming languages and scripts. Since this simulation work is relatively expensive, with limited local computing resources at hand, efforts should be put to collect the distributed machine resources around, and plug them in through network when they are available and unplug them out whenever they need to quit with minimum interference of the running optimization and the machines' current environments. The Python is capable to run on most of the operating systems so that the platform developed in this work is compatible with Mac OS, Windows and Linux systems, and the optimization work can be loaded by the cross-platform computing. Besides that, Python also provides first-rate interfaces to other programming languages and scripts like C++, Bash shell and is of the capability to couple them together to implement various tasks at different level from formatted i/o to Monte Carlo Method to machine communication. Generally, in this framework, the base layer is a parallel computing module which provides universal tasks dispatching service. Along with the tasks dispatcher module, the tasks generator module and the task implementing module are joined together to accomplish the whole optimization work. In the following subsections, the development of the tasks dispatcher module, the "Slave" module and the tasks generator module are introduced.

3.3. Tasks Dispatcher Module

The parallel computing module presenting its nickname as "Slavemaster" in the

framework is developed based on Pyro4 package in Python. This module functions in the way of a universal tasks dispatcher which means it can receive any type of tasks from tasks generator modules and assign the tasks to worker modules (Slaves) as shown in figure 3-2. Because of the central role of this module, it should always be available before other modules initiate their activities. Otherwise, the functional modules will fail to shake hand with the Slavemaster, then the framework cannot be coordinated. The connection between the functional modules with Slavemaster starts from shake-hand process in which they find each other. Once the shake-hand successes, task generator can turn over its tasks to Slavemaster continuously or intermittently. And since then, the Slavemaster will take charge of the tasks until the task-result pairs are returned back to tasks generator for further processing.

Inside the Slavemaster, the tasks bank is a collection of tasks received. It follows the first in first out rule of queue type. Once a task is allotted to a Slave, it will be removed from tasks bank and stays in waiting-products list until the results are returned from Slave. However, not all the tasks should be implemented, since the same tasks may have been executed in history. Thus, results of these tasks can be pulled from an archive of the historical data instead of assigning them again. Consequently, the archive of implemented tasks plays an important role to avoid redundant work in this optimization. The message passing between the tasks dispatcher module and functional modules are through the network. The Slavemaster exposes a single instance of its class through IPv4 to the internet. Then the functional modules can approach it and send messages to the Slavemaster. Usually in the time span of an optimization, the Slave nodes could crash (die) or quit the framework for

some reason. Thus, the Slave status monitoring, tasks recovery and reassignment functions are periodically implemented by the daemon process.

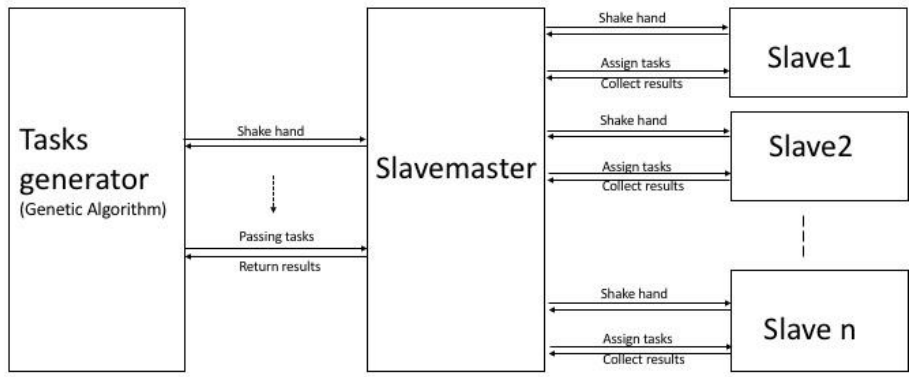

Figure 3-2 Tasks dispatcher module

3.4. Slave Module

In the evolutionary optimization, unlike a brute force design, it saves significant time of the exploration of the input vector space. However, expensive simulation still cannot be evaded. The load is mainly taken on the shoulder of the functional module which is called “Slave” shown in figure 3-3.

In the slave module, the neutronics and thermal-hydraulics modules are integrated. The neutronics module takes the raw input parameters vector from the Slavemaster, then translate it into reactor geometry and fuel composition parameters. With these parameters, input file is generated for McCARD(Shim, Han, Jung, Park, & Kim, 2012), and the running is triggered.

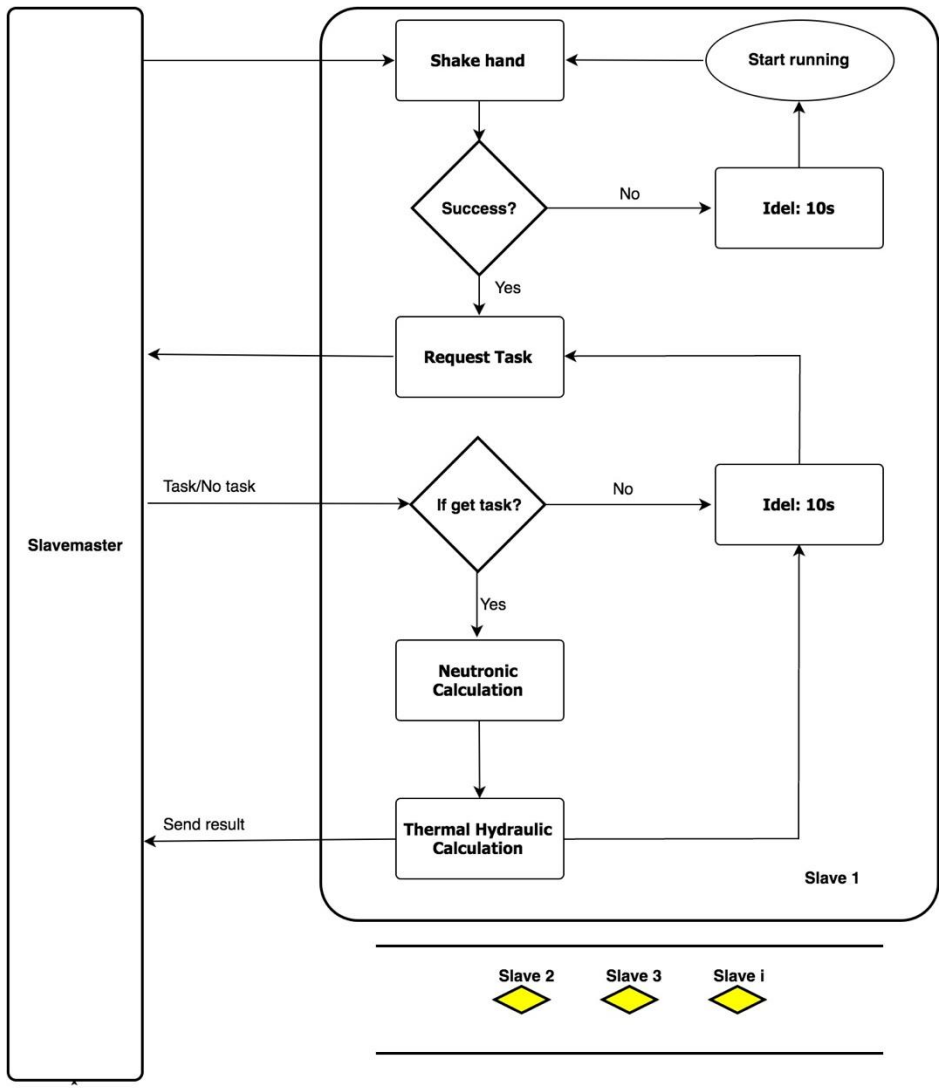

Figure 3-3 Slave module

The fuel rod with the maximum linear power is treated as the hot fuel rod, and its linear power distribution is transferred to the Single Pin Cell module as one of the input parameters in thermal hydraulic calculation to determine the maximum fuel temperature and cladding temperature. In this thermal hydraulic module, the input parameters are used to generate system components nodes which can determine the

system pressure drop if the mass flow rate is given. While in natural circulation function, it can determine the mass flow rate when the loop pressure drop is given. Thus, by iteration, the system pressure drop and mass flow rate are determined. The inlet temperature, outlet temperature, linear power array and geometry of the fuel pin and coolant duct are used in the heat transfer calculation.

3.5. Genetic Algorithm Module

The Genetic Algorithm module is one of the core modules which controls the optimization calculation direction. The implementation flowchart of this module is shown in figure 3-4.

As the start of the process, an initial population is generated randomly in the searching space. After that, these inputs are sent to tasks dispatcher module and then idles until the feedback has been received successfully. After the results data have been returned, they are compared with the chosen Pseudo-local-optimum objective values shown in table 3-1 to evaluate the phenotype of each individual. According to the number of objectives, the phenotype which is a list with four elements, is marked as 1 in the ith element if it dominates the chosen solution in objective i, otherwise, the corresponding element is marked as 0. The individual's phenotype rank is the summation of the phenotype list, so it represents the overall quality of this individual which means that the higher rank individual dominates the chosen solution in more objectives. In the process of selection in SPP, the selected probability of one individual is calculated by its rank divided by the overall rank of the population. Thus, the higher rank of the individual will have a higher possibility

to be selected. In this way, the probability of one individual to be selected is related to its own rank as well as the ranking distribution in current generation. In order to maintain the diversity of the population, in the archive, the selection probability is determined by the genotype dissimilarity. The genotype dissimilarity of an individual is also a summation of a four-element list that each element counts the number of the archived members having a different value of this element in the input vector. The higher genotype dissimilarity individuals have the higher probability to be selected.

Table 3-1 The chosen Pseudo-Local-Optimum Input Parameters and Objective Values

The chosen Pseudo-Local-Optimum Input Parameters			
Fuel Pellet Diameter [cm]	Fissile Material Fraction	Core Inlet Temperature [K]	Length of Riser [m]
2.363	0.2	713.15	1.9
The chosen Pseudo-Local-Optimum Objective Values			
BOL Effective Criticality	Primary Side Outlet Temperature [K]	Fast Neutron Flux Ratio	Reactor Height (active core + upper plenum + riser length) [m]
1.1515	830.96	0.561	4.3

In the mating process, the survived individuals in the selection process are chosen randomly to be the fathers and mothers then the multi-points crossover is applied. The partition of crossover points are randomly selected by crossover possibility factor, the independent variables in the chromosomes in real-value encoding are copied to each other's chromosome, so at these stage, the variables in mother and father are partially interchanged. In this offspring generating process, new chromosomes of the same size as previous generation population are produced. Immediately after a new chromosome has been hatched, it goes through the mutation

process controlled by mutation possibility factor that certain number of the points in chromosome are selected and mutated to random values in the searching space. After having completed the selection, crossover and mutation, the routine brings the process back to the start point of the process.

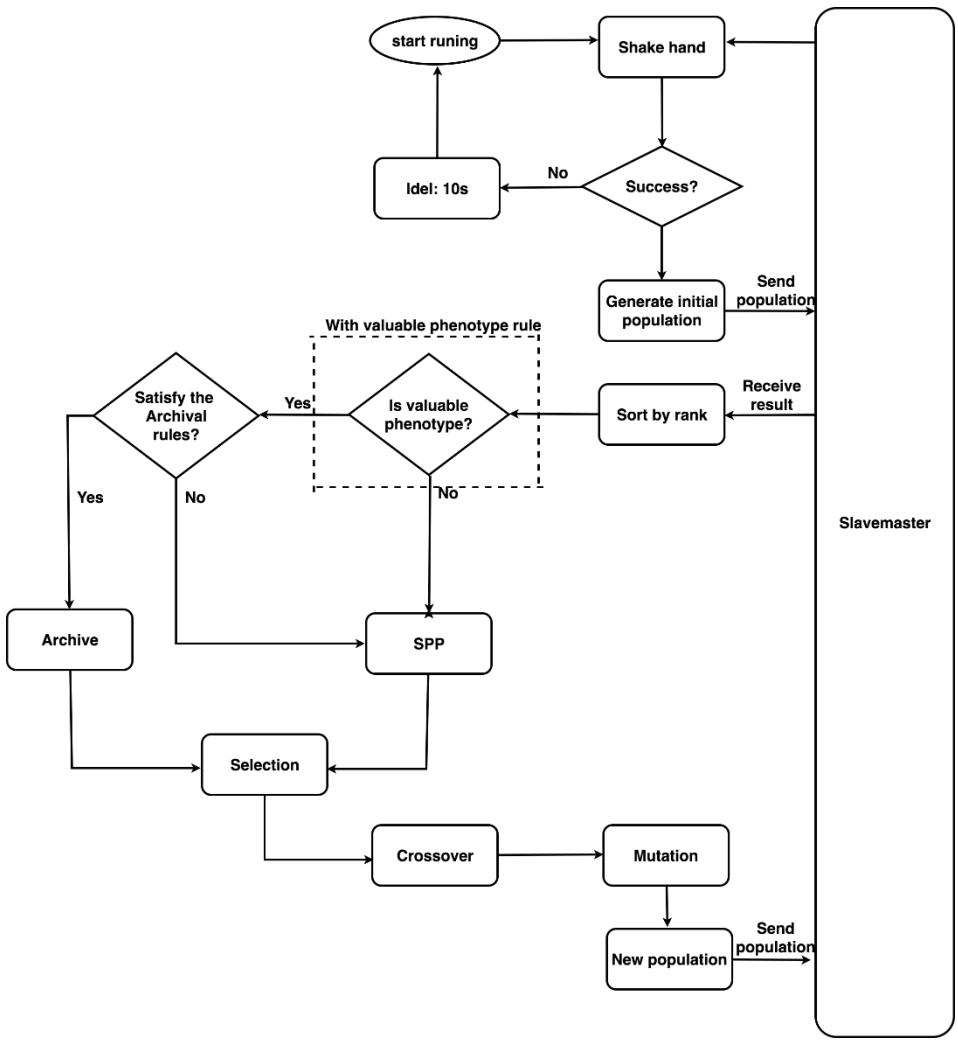

Figure 3-4 Genetic Algorithm module

4. Neutronics Submodule

Neutronics Submodule is one of the submodules in the Slave module. In this chapter, the neutronics analysis setup, reactor core layout, material composition used in this submodule are presented and the parametric survey are conducted.

4.1. Simulation Setup

The neutronic design is conducted by using McCARD which is developed in SNU. It solves the continuous energy neutron transport equations using Monte Carlo method (Shim et al., 2012). The ENDF/B-VII.0 temperature dependent cross section libraries are used in this study. The validation of the McCARD was widely examined by International Handbook of Evaluated Criticality Safety Benchmark Experiments from thermal spectrum to fast spectrum critical experiments fueled with Uranium and Plutonium while the depletion calculation of McCARD was validated with various codes like CASMO, HELIOS, and MVP-BURN (Shim et al., 2012)(Tak, Lee, & Kim, 2013)(Edenius, Ekberg, Forssén, & Knott, 1995)(Stamm'ler, 1998)(OKUMURA, MORI, NAKAGAWA, & KANEKO, 2000).

To guarantee the precision at the acceptable level. The relative standard deviation is kept within 0.001 in each calculation with 20,000 particles and 25 inactive cycles and 75 active cycles. In depletion calculation, the time bin is chosen to be 0.5 years. In each fuel pin, totally 9 layers are used axially to tally central pin fission power distribution. The normal surface conditions are used on reactor core boundary which means neutrons across the reactor boundary is treated as leakage.

4.2. Layout of BORIS Core

In the neutronic calculation, the diameter of fuel pin and the Pu-MA fraction is optimized. The total fuel volume, cladding thickness, fuel bonding gap and pitch are maintained the same as the chosen pseudo-local-optimum. Thus, with the change of fuel pellet diameter, the length of fuel pin changes correspondingly. The length of the upper plenum is twice as the height of the active core, which is considered as conservative from previous study (Hyung M. Son & Suh, 2014). The pitch-to-diameter ratio varies in different fuel pellet diameter also. Triangular fuel lattice of totally 757 fuel rods with the pitch value as 30.8 mm are used in reactor core as shown in figure 4-1. The length of axial reflectors is 20 cm located above and below the fuel pellets. The radial reflectors and control rods are not considered in preliminary design and they are not bred in this work. Since the lack of radial reflector, to make the reactor can maintain critical for successive 20 years, the diameter of the coolant is doubled to take the role of radial reflector. The fuel rods lattice is arranged to minimze diameter from the core center to its boundary circle using the rule provided by A.P. Fraas et al. (FRAAS & OZISIK, 1965). In this rule, the circles enclosing the fuel rods start from the center of the core, then the next ring is formed by increasing the circle radius until the next outer layer of rods' center are crossed by the circle. By implementing this method, totally 69 layers are enclosed.

4.3. Material Composition

4.3.1. U-Pu-MA-N

The U-Pu-MA-N is used in the BORIS due to its excellent performance of

conductivity and high melting point as well as the wide solubility between uranium/plutonium nitride and minor actinide nitride with NaCl type structure (Muta, Kurosaki, Uno, & Yamanaka, 2008). The fuel composition for preliminary design is shown in table 4-1 (Buongiorno et al., 2001). The fuel density is assumed to be 85% of theoretical density 14.567 g/cm^{2}which gives 12.345 g/cm^2 (Hyung M. Son & Suh, 2014).

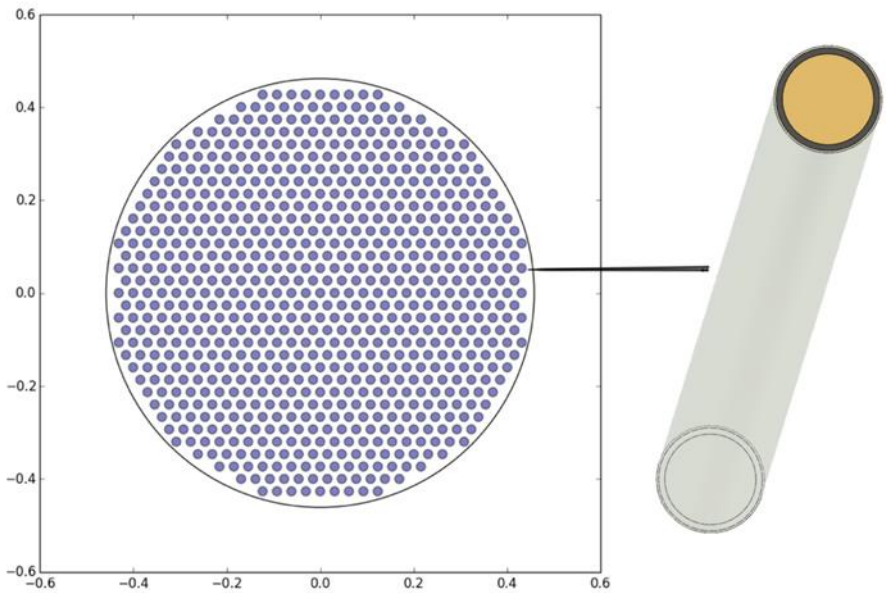

Figure 4-1 Whole core layout

4.3.2. Lead

The natural lead is used as reactor coolant and in fuel bonding gap. The composition of natural lead is shown in table 4-2. The density of Lead in neutronics calculation is an average density based on the average temperature taken from the preliminary design which is 10.445 g/cm^2(Hyung M. Son & Suh, 2014).

4.3.3. HT9

The HT9 is used as cladding material as well as the axial reflector material. The constitution of HT9 is shown in table 4-3, and each isotope is in its natural element composition. The reference density of HT9 is taken as 7874 kg/m2 (Hyung M. Son & Suh, 2014)(Leibowitz & Blomquist, 1988).

Table 4-1 U-Pu-MA-N weight fraction

Fuel Composition Data for Pu-MA-U-N Fuel							
Nuclide	U-235	U-238	Pu-238	Pu-239	Pu-240	Pu-241	Pu-242
Weight Fraction [%](91% U, 9%Pu)	0.52	73.98	0.32	9.28	4.16	1.6	0.64
	74.5		16				
Nuclide			Np-237	Am-241	Am-243	Cm-244	N-15
Weight Fraction [%]			1.72	1.8	0.36	0.12	5.5
			4				5.5

Table 4-2 Coolant and fuel bonding gap natural lead composition

Natural Lead Composition					
Nuclide	Pb-204	Pb-206	Pb-207	Pb-208	TOTAL
Weight Fraction [%]	1.4	24.1	22.1	52.4	100

Table 4-3 Fuel cladding HT9 composition

HT9 Composition						
Elements	Each constituting isotopes are in natural fractions					
	C	Cr	Fe	Ni	Mn	Mo
Weight Fraction [%]	0.2	12	84.85	0.5	0.2	1
Elements	Si	P	S	V	W	TOTAL
Weight Fraction [%]	0.25	0	0	0.5	0.5	100

4.4. Parametric Survey and Design Domain

In this section, the parametric survey is conducted regarding the Pu-MA fraction and the fuel pellet diameter in neutronic aspect. In order to avoid the unaffordable depletion calculation in the evolution process, the designing boundary should be identified. The figure 4-2 presents the value of Keff with respect to the variation in the fuel pellet diameter and the Pu-MA fraction. From this figure, it can be observed that, with the increase of Pu-MA fraction and Fuel pellet diameter, the BOL Keff increases due to the higher fissile material fraction and lower height of reactor core which is more compact that decreases the neutron leakage. The blue region in the figure illustrates the reactor core is subcritical at the beginning of life. In this region, either Pu-MA fraction is low or/and fuel pellet diameter is thin. Therefore, this region should not be considered in designing. The yellow region represents the reactor can be critical at the beginning of life but cannot sustain to 20 years. Thus, the yellow region is also not in the design domain. The red region illustrates the design domain of Pu-MA fraction and fuel pellet diameter because the effective criticality is above 1 at BOL and at EOL. The design domain boundary is fitted shown in figure 4-3. This coarse boundary can be expressed by:

$$D_p = 262.24 \times Frac^4 - 237.18 \times Frac^3 + 80.253 \times Frac^2 - 12.106 \times Frac \quad (4.1)$$

The R of this polynomial fitting is 0.9928.

Some facts can be extracted from figure 4-2 and figure 4-3 in the optimization. According to the design objective 1 to minimize the BOL Keff for the sake of

excessive reactivity, it is desired to place the parameters as close as possible to the design boundary where there is the lower Pu-MA fraction or/and thinner fuel pellet. On the other hand, decreasing the fuel rod diameter will induce the higher core height so that the reactor tends to be less compact. So, a thicker fuel pellet diameter is desired to cater the objective 4 of the compactness of the reactor.

In order to characterize the neutron spectrum, the neutron flux is tallied with a cutting energy of 0.1 MeV. The fast neutrons fraction is represented by the ratio of neutrons with energy above this value. From figure 4-4 and figure 4-5, it shows with the increase of P/D or with the decrease of Pu-MA fraction, the fast neutrons fraction is decreasing. The reason is that the wider space between the fuel rods provide more chances for neutrons to be moderated and the decrement of the fissile material induces the total absorption cross section reduction; thus, the life time of neutrons increase and more moderations take place.

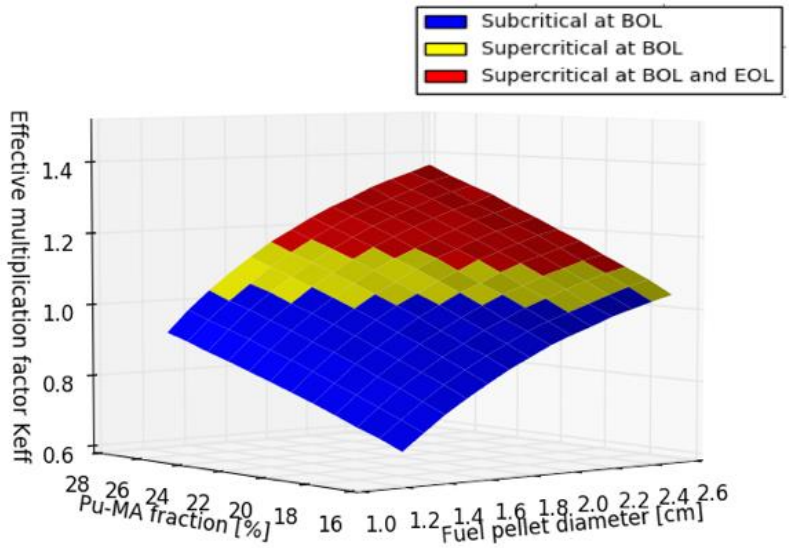

Figure 4-2 Keff v.s. Pu-MA fraction and fuel pellet diameter

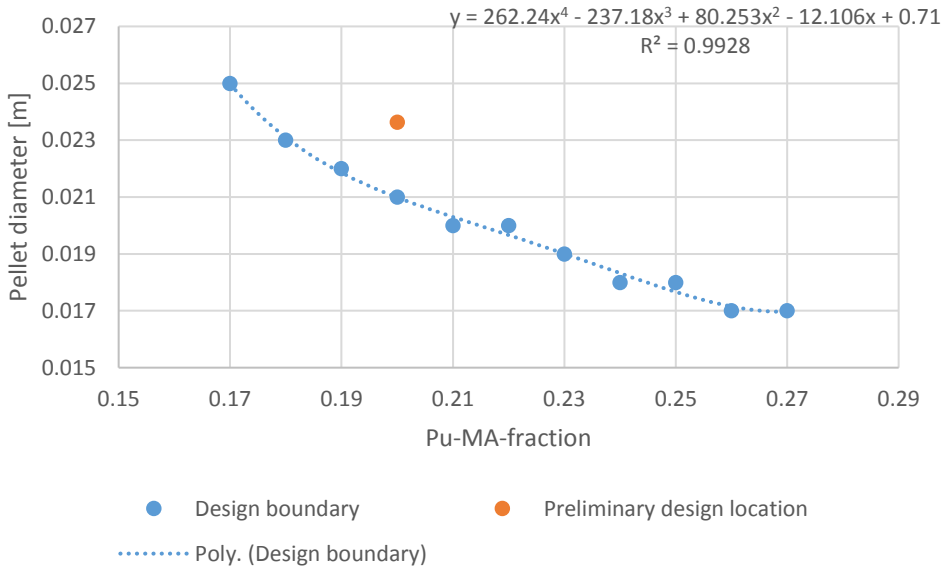

Figure 4-3 Neutronics design domain

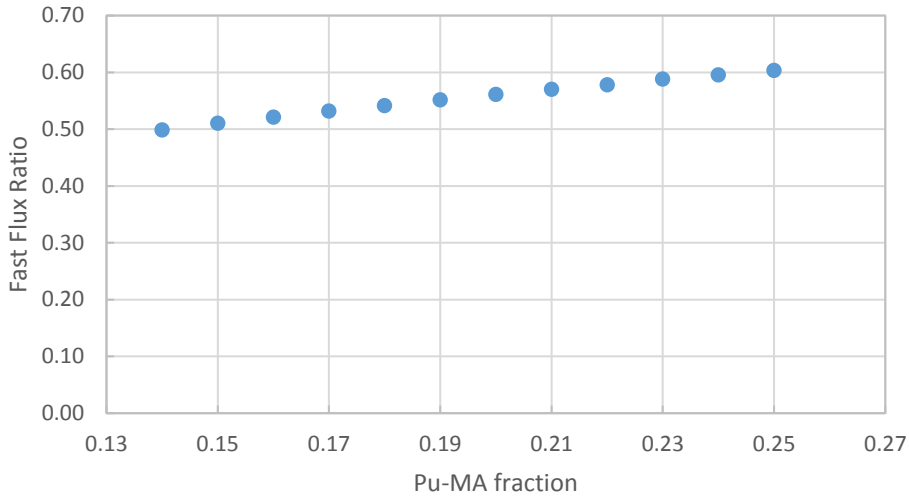

Figure 4-4 Fast flux ratio vs Pu-MA fraction (P/D=1.1)

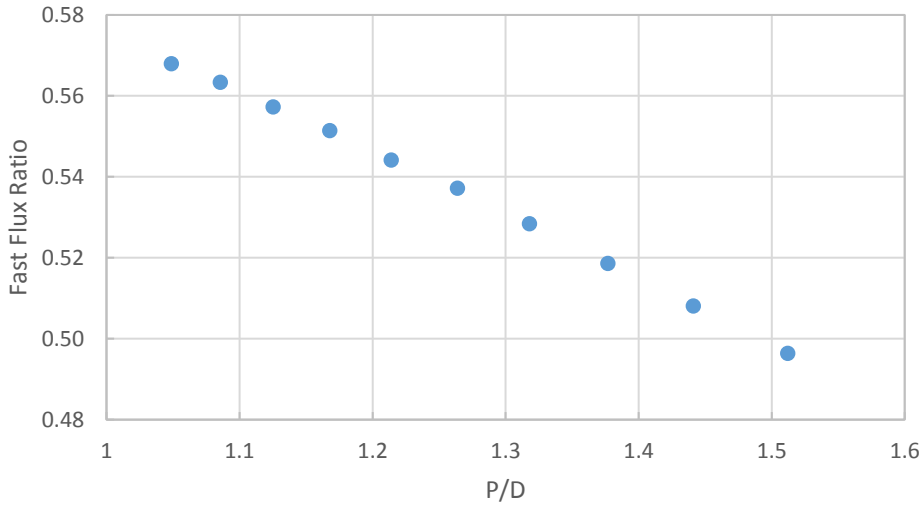

Figure 4-5 Fast flux ratio vs P/D (Pu-MA fraction =20%)

5. Thermal-Hydraulics Submodule

In this section, the thermal-hydraulics submodule is developed and validated; the parametric survey is conducted to investigate the influence of optimized parameters on the behavior of the BORIS system.

In this thermal-hydraulic submodule, the full core natural circulation analysis and the hot pin cell analysis are conducted. In the natural circulation, the reactor core performs as the heat source while the mounted heat exchangers serve as the heat sink. The channels between them are called hot leg and cold leg. The considerable temperature difference between the hot leg and the cold leg causing large density change generates the continuous driving force to balance the hydraulic resistance. By giving geometry of the reactor, the power of the reactor and the inlet temperature, the mass flow rate and outlet temperature can be calculated by iteration. This outlet temperature along with other parameters will, then, be applied as the input parameters to hot pin cell analysis. A hot pin cell is the pin cell shown in figure 5-1, which has the most fission energy deposition. In the hot pin cell analysis, a standard heat transfer calculation is performed in which the deposited heat in fuel pin transfers across the fuel region itself, then pass across the liquid lead fuel bonding, the HT9 cladding and finally reach the bulk of coolant. The enthalpy rise in the hot channel is assumed to be the same as average channels. In reality, to achieve this uniform enthalpy rise distribution, the distributors should be well-designed in zone-by-zone orificing optimization (Zhao, Tso, & Tseng, 2011).The axial heat transfer though is of importance in liquid metal alloy coolant, however when compares with radial heat

transfer, a minor effect is assumed due to the less temperature gradients. Thus, it is not applied in this calculation. It should be noted that for more accurate calculation, this effect should not be ignored. The contents following will be describing the mechanisms used in the calculation.

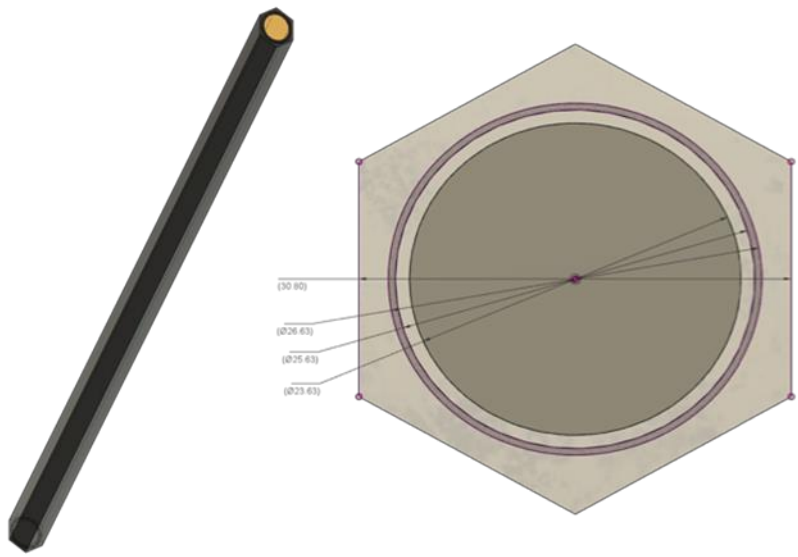

Figure 5-1 Hot pin cell

5.1. Governing Equations

5.1.1. Energy conservation and mass conservation equations

Reactor Energy Balance Equation under steady state condition:

$$Q - \dot{q} = C_p(T_{out})\dot{m}_{out}T_{out} - C_p(T_{in})\dot{m}_{in}T_{in} \quad (5.1)$$

Where, Q is the reactor thermal power which is assumed to be 22.2 MWt, T_{in} and T_{out} are inlet and outlet temperature separately. Assuming the adiabatic boundary condition, $\dot{q} = 0$, and that these is no bypass in reactor, the mass flow rate at the inlet and the outlet should have the same value:

$$\dot{m} = \dot{m}_{in} = \dot{m}_{out} \tag{5.2}$$

Finally, the outlet temperature can be expressed by,

$$T_{out} = \frac{Q + C_p(T_{in})\dot{m}T_{in}}{C_p(T_{out})\dot{m}} \tag{5.3}$$

By iteration, the outlet temperature can be determined.

5.1.2. Loop momentum conservation equation

Loop Momentum conservation equation under steady state condition is:

$$\beta g \rho_0 \Delta T L_{th} = \Delta P \tag{5.4}$$

where β is coolant expansion coefficient, g is gravity acceleration, ρ_0 is reference coolant density, ΔT and L_{th} are the temperature difference and the elevation difference between hot center and cold center, ΔP is the total pressure drop due to hydraulic resistant in loop. The overall pressure drop is counted by the summation of pressure drop of each component (Hyun et al., 2011):

$$\Delta P = \frac{1}{2}\rho \sum_i V^2 \left(f\frac{L_i}{D_h} + K\right)_i \tag{5.5}$$

Where V is reference velocity, D_h is hydraulic diameter, L_i is length of the i-th component, f is fraction factor, K is form loss coefficient. The Darcy-Weisbach friction factor models are utilized in this equation:

$$f = \frac{64}{Re} \quad \text{for} \quad 0 < Re \leq 2200 \tag{5.6}$$

$$f = \left(3.75 - \frac{8250}{Re}\right)(f_{Re=3000} - f_{Re=2200}) + f_{Re=2200} \quad \text{for} \quad 2200 < Re \leq 2200 \tag{5.7}$$

$$\frac{1}{\sqrt{f}} = -2\lg\{\frac{\varepsilon}{3.7D_h} + \frac{2.51}{Re}[1.14 - 2\lg(\frac{\varepsilon}{D_h} - \frac{21.25}{Re^{0.9}})]\} \quad \text{for} \quad Re \geq 3000 \tag{5.8}$$

The form loss coefficients used in this study are sudden expansion or

contraction, orifices, elbow, spacers. These formulas are validated by HELIOS experiment facilities (Hyun et al., 2011), except for the formula in grid spacer which has been studied by Chen et al. for the validation case in later section (Chen & Suh, 2016), and here the correlation from Schikorr et al. is used (Schikorr, Bubelis, Mansani, & Litfin, 2010).

For a sudden expansion, the Equation 5.9 is applied:

$$K = \left(1 - \frac{A_1}{A_0}\right)^2 \tag{5.9}$$

For a sudden contraction, the empirical loss coefficient is (Massey & Ward, 1998):

$$K = 0.5 - 0.7\left(\frac{A_0}{A_1}\right) + 0.2\left(\frac{A_0}{A_1}\right)^2 \tag{5.10}$$

Where A_1 is upstream area and A_0 is downstream area.

For an elbow shown in figure 5-2, the form loss coefficient is calculated by (H Nippert, 1929):

$$K = K_{\mathrm{Re}} \cdot K_{loc} + K_{\mathrm{fr}} \tag{5.11}$$

$$K_{\mathrm{fr}} = 0.0175 \cdot \frac{R_o}{D_o} \cdot \Phi \cdot \lambda \tag{5.12}$$

$$K_{\mathrm{loc}} = A_1 \cdot B_1 \tag{5.13}$$

Where A_1 and B_1 are taken from table 5-1 and table 5-2; K_{Re} is shown in table 5-3.

Table 5-1 Values of A_1 for elbow form factor

δ	20.0	30.0	45.0	60.0	75.0
A_1	0.31	0.45	0.60	0.78	0.90
δ	90.0	110.0	130.0	150.0	180.0
A_1	1.00	1.13	1.20	1.28	1.40

Table 5-2 Values of B_1 for elbow form factor

R_0/D_0	0.50	0.60	0.70	0.80	0.90
B_1	1.18	0.77	0.51	0.37	0.28
R_0/D_0	1.00	1.25	0.50	2.00	4.00
B_1	0.21	0.19	0.17	0.15	0.11

Table 5-3 Values of K_{Re} for elbow form factor

Values of K_{Re}						
	$Re \times 10^{-5}$					
R_0/D_0	0.10	0.14	0.20	0.30	0.40	0.60
0.5-0.55	1.40	1.33	1.26	1.19	1.14	1.09
>0.55-0.70	1.67	1.58	1.49	1.40	1.34	1.26
>0.70	2.00	1.89	1.77	1.64	1.56	1.46
	$Re \times 10^{-5}$					
R_0/D_0	0.80	1.00	1.40	2.00	3.00	4.00
0.5-0.55	1.06	1.04	1.00	1.00	1.00	1.00
>0.55-0.70	1.21	1.19	1.17	1.14	1.06	1.00
>0.70	1.38	1.30	1.15	1.02	1.00	1.00

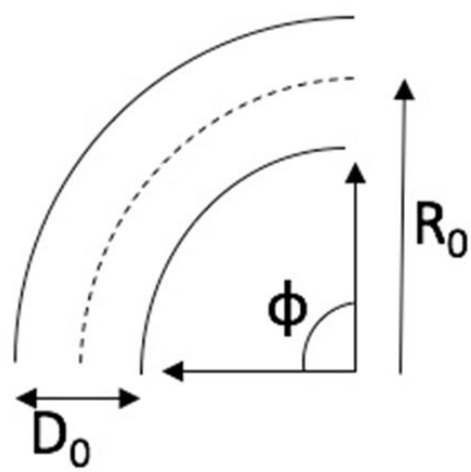

Figure 5-2 Elbow

For an orifice shown in figure 5-3, the form loss coefficient is (Idelchik, 1953):

$$K = \left(\frac{F_1}{F_0}\right)^2 \left(1 + 0.707\sqrt{1 - \frac{F_0}{F_1}} - \frac{F_0}{F_1}\right)^2 \quad (5.14)$$

Where, F_1 is upstream flow area, F_2 is the downstream flow area, F_0 is the abrupt contracted flow area.

The form loss coefficient in the region of grid spacers is determined from the equations 5.15 and 5.16 (Schikorr, Bubelis, Mansani, & Litfin, 2010):

$$K = Cv \times \epsilon^2 \quad (5.15)$$

$$Cv = MIN[2.5 + \frac{73.14}{Re^{0.264}} + \frac{2.79 \times 10^{10}}{Re^{2.79}}, \frac{2}{\epsilon^2}] \quad (5.16)$$

Where ϵ is the blockage ratio. Typically ranges from 0.5 – 1.5.

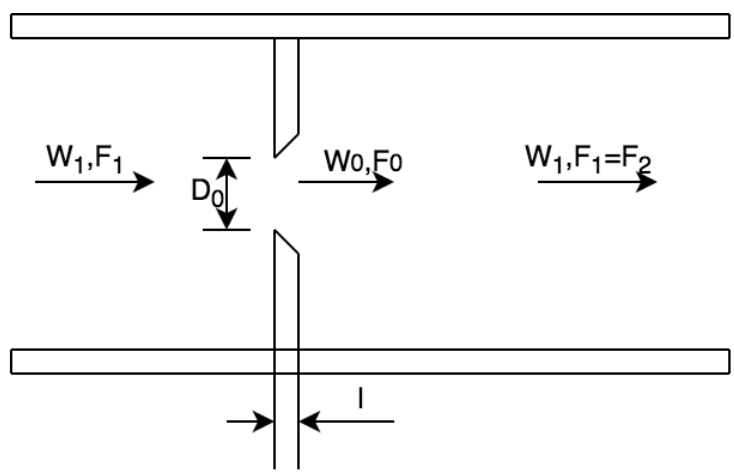

Figure 5-3 Orifice

5.1.3. Heat transfer equations

In the hot pin cell calculation, the steady-state temperature distribution is derived in 2-dimentional space. The radial variation is affected by the power

generation from the fuel region while the axial variation is affected by both the power generation and coolant flow.

The temperature variation in coolant bulk, cladding outer surface, cladding inner surface, fuel outer surface and fuel center are calculated from equation 5.17 to equation 5.20:

$$T_{clad_o} = T_{coolant\_bulk} + \frac{q_l}{\pi D_r h} \tag{5.17}$$

$$T_{clad_i} = T_{clad_o} + \frac{q_l}{2\pi\lambda_{HT9}} \ln \frac{r_{clad_o}}{r_{clad_i}} \tag{5.18}$$

$$T_{fuel_o} = T_{clad_i} + \frac{q_l}{2\pi\lambda_{Lead}} \ln \frac{r_{clad_i}}{r_{fuel}} \tag{5.19}$$

$$\mathrm{T_{fuel_c}} = \mathrm{T_{fuel_o}} + \frac{\mathrm{q_l}}{4\pi\lambda_{\mathrm{fuel}}} \tag{5.20}$$

Where the thermal conductivity of HT9 is (Leibowitz & Blomquist, 1988):

$$\lambda_{\mathrm{HT9}} = \begin{cases} -1.696 \times 10^{-5}\mathrm{T}^2 + 2.428 \times 10^{-2}\mathrm{T} - 1.696 \times 10^{-5}\mathrm{T}^2, \lambda < 0 \\ 12.027 + 1.218 \times 10^{-2}\mathrm{T} \quad , \lambda \geq 0 \end{cases} \tag{5.21}$$

The thermal conductivity of Lead is (Pacio, 2015) :

$$\lambda_{\mathrm{Lead}} = 9.2 + 0.011 \times \mathrm{T} \tag{5.22}$$

The Nusselt number is calculated by the correlation proposed by Cheng etc. based on the existing models and CFD results for Lead Bismuth coolant (Cheng & Tak, 2006):

$$\mathrm{Nu} = \mathrm{A} + 0.018\mathrm{Pe}^{0.8} \tag{5.23}$$

Where

$$A = \begin{cases} 4.5 & Pe \leq 1000 \\ 5.4 - 9 \times 10^{-4} Pe & 1000 \leq Pe \leq 20 \\ 3.6 & Pe \geq 2000 \end{cases}$$

5.1.4. Coolant property correlations

The density and heat capacity depended on temperature is taken from the handbook from the OECD/NAE (Pacio, 2015).

$$\rho_{Pb} = 11367 - 1.1944 \times T \tag{5.24}$$

$$C_{p_{pb}} = 175.1 - 4.961 \times 10^{-2} \times T + 1.985 \times 10^{-5} \times T^2 - 2.099 \times 10^{-9} \times T^3 - 1.524 \times 10^{6} \times T^{-2} \tag{5.25}$$

5.2. Model Validation

5.2.1. Case description

Calculations of two benchmarks of Lead-Alloy Cooled Advanced Nuclear Energy System (LACANES) experiment (Hyun et al., 2011) in isothermal steady state forced convection and in natural circulation are conducted to assess the exactness of the developed code. The experimental data for LACANES was produced by a Lead-Bismuth thermal-hydraulic loop, HELIOS, in twenty meters high (Hyun et al., 2011). The experimental facility is simply described in the following paragraph, more details can be found in the benchmark report (Hyun et al., 2011).

This loop consists of a core, an expansion tank, a heat exchanger, a mechanical pump, an orifice, five gate valves, nine tee junctions with eight straight flow directions and one branch flow direction, nine 45º elbows, four 90º elbows and around 14.9 meters long straight pips. In these experiments, the pressure drop data were only measured in core region, orifice region, gate valve region and heat

exchanger region. The regions without experimental data, the CFD result was taken as the supplementary. The differential pressure transducers and thermocouples' position are shown in figure 5-4. The loop can switch its operation mode between forced convection and natural convection by utilizing the parallel bypass of the mechanical pump. In natural convection, the mechanical pump component pipeline is fully closed and the bypass pipeline is fully opened while running in forced convection, the openings is reversed. The thermal centers elevation difference is 7.4 m and the maximum power in core region is 60 kW in natural circulation mode.

5.2.2. Validation Results

The validation results of isothermal steady-state forced convection and natural circulation are presented in table 5-4 and table 5-5. The maximum relative error appears in the gate valve region at high coolant mass flow rate case which is 11.6 % and core region at low mass flow rate case which is -9.55 % in forced convection benchmark. The accuracy of pressure drop correlation is a widely existing problem in most prediction studies, and practically a scaled-down model need to be constructed before a prototype experiments. The overall pressure loss prediction under various mass flow rate is given in figure 5-5 which fits the experimental data well. In natural convection case, the relative errors of hot leg temperature and mass flow rate are 0.37% and 0.78% separately. They are considered to be excellent. Thus, the results from this code is considered to be acceptable in case of conceptual design.

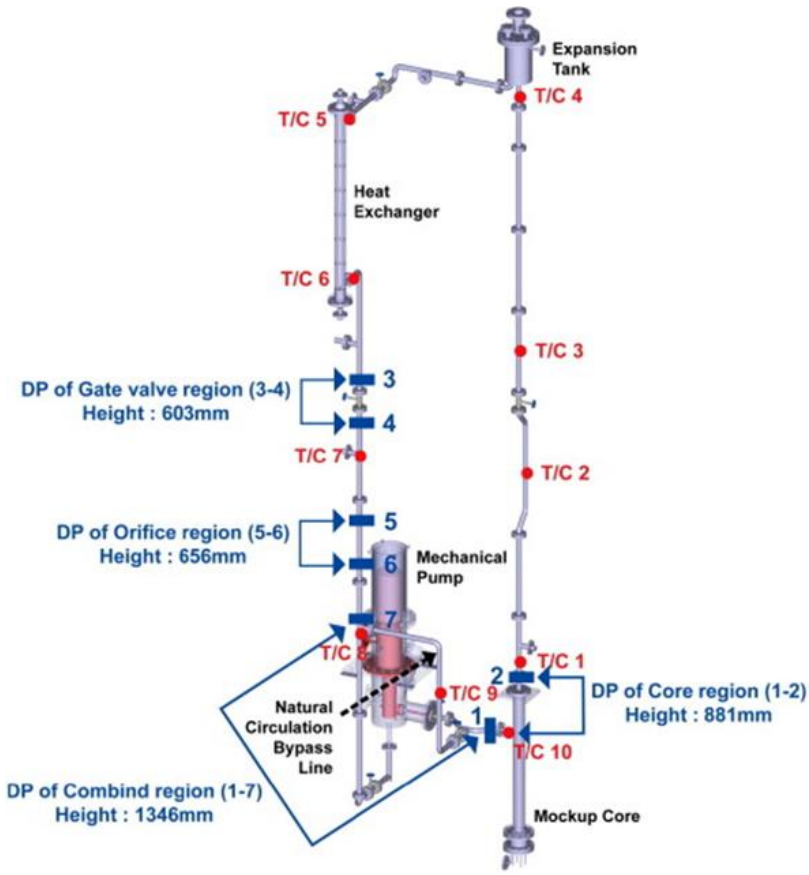

Figure 5-4 Three-dimensional diagram of the HELIOS forced convection test setup (Hyun et al., 2011)

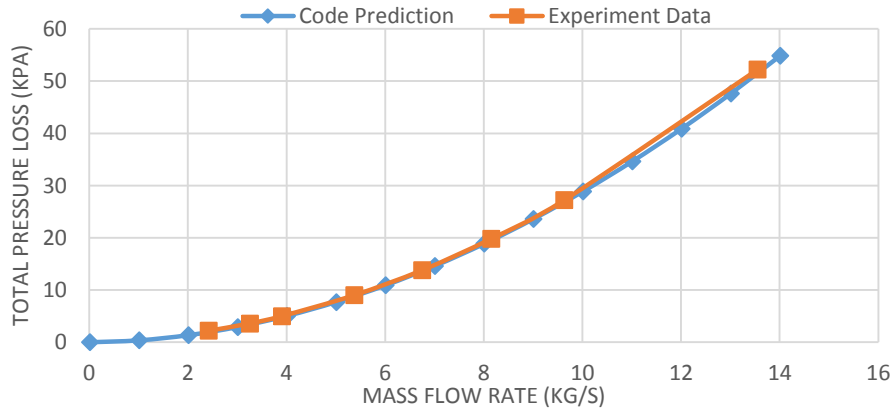

Figure 5-5 Total pressure loss vs mass flow rate

Table 5-4 Code validation results of isothermal steady state forced convection

Parameters		LACANES benchmark	The developed code	Relative error (%)
Coolant mass flow rate (kg/s)		13.57		-
Pressure loss (kPa)	Core region (measured)	52.491	51.607	-1.68
	Gate valve region (measured)	3.025	3.377	11.6
	Orifice region (measured)	20.247	19.358	-4.39
	Total pressure loss (measured + cfd)	113	112.568	0.38
Coolant mass flow rate (kg/s)		3.27		-
Pressure loss (kPa)	Core region (measured)	3.781	3.420	-9.55
	Gate valve region (measured)	0.182	0.196	7.69
	Orifice region (measured)	1.194	1.129	-5.44
	Total pressure loss (measured + cfd)	-	7.333	-

Table 5-5 Code validation results of natural convection

Parameters	LACANES benchmark	The developed code	Relative error (%)
Core heat (kW)	18.3	Benchmark value	-
Coldleg temperature (K)	519.35	Benchmark value	-
Hotleg temperature (K)	570.35	568.22	0.37
Mass flow rate (kg/s)	2.54	2.56	0.78

5.3. Parametric Survey

In this section, the parametric analysis is conducted to obtain the characterization of the influence of the optimized parameters on the thermal-hydraulic and heat transfer behavior of the system.

The figure 5-6 shows the influences of the Pu-MA fraction on the maximum fuel center temperature, maximum cladding temperature and outlet temperature of the primary side. In the range of 20 percent to 27 percent of the Pu-MA fraction, the temperatures are not presented to be relevant to this fraction. The same irrelevance relationship between the Pu-MA fraction and the whole core mass flow rate and the maximum velocity is also observed from the figure 5-7. With the constant core inlet, core outlet temperature and core geometry, neither the hydraulic resistance nor the driving force changes signigicantly. The only factors influence the variation of the system's behavior is the linear power distribution and the thermal conductivity of the fuel pellet. However, the influence is not strong enough to cause an obvious effect. So, there is only a slight fluctuation of the system's behavior presented.

The figure 5-8 shows the influence of the fuel pellet diameter. All of these temperatures distributed in fuel, cladding and coolant increase as the fuel pellet diameter increases. The reason is that when the fuel pellet diameter becomes thicker, the coolant flow area between fuel rods bundles decrease correspondingly. Thus, the heat removal ability decreases by the increasing hydraulic resistance. The effect can be demonstrated by the facts shown in the figure 5-9. The whole core mass flow rate declines gradually with the growth of the fuel pellet diameter, though the maximum velocity inside smaller channel increases. Since, it is desirable to hold a lower

cladding temperature and fuel center temperature, the thinner fuel pin is appreciated. However, the higher primary side temperature can increase the thermodynamic efficiency, thus a thicker fuel pin is favored for this sake.

The figure 5-10 presents the influence of the length of riser on the temperature distribution. As the length of riser increases, the driving force induced by the gravity increases. Thus, both the mass flow rate and maximum velocity in fuel bundles can be relatively higher, when the riser is longer as shown in the figure 5-11. Consequently, the temperatures in fuel center, the cladding and the outlet temperature will be lower when increasing the riser length. From the objectives of the design, a longer riser is favored to cater the limitation of the fuel and cladding temperature but disfavored by the objective to increase the outlet temperature in primary side as well as the compactness of the reactor.

The figure 5-12 illustrates the influence of the inlet temperature on the temperature distribution. All of the temperatures in the fuel, cladding and coolant bulk increases because of the inlet temperature increases under the constant power in the reactor core. It is a beneficial effect for thermodynamic efficiency, but not desired for the safety concern. The whole core mass flow rate and the maximum velocity also increase with the inlet temperature increase slightly, which signifies that the natural circulation is enhanced as shown in figure 5-13.

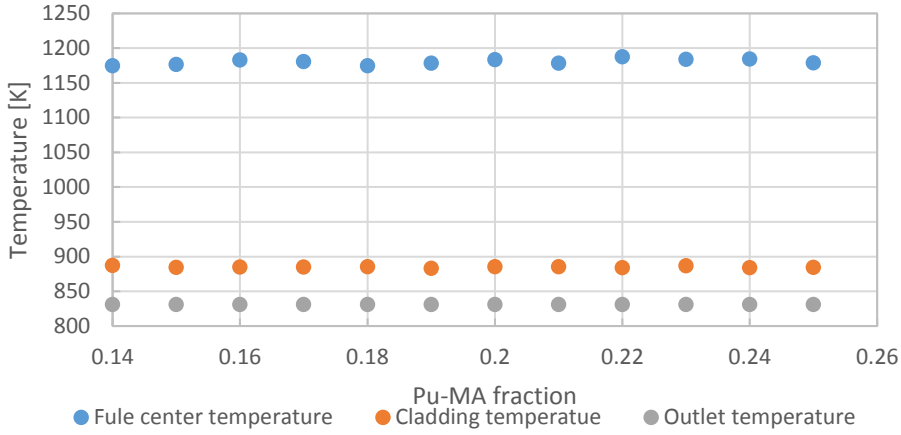

Figure 5-6 Influence of Pu-MA fraction on the fuel center temperature, cladding temperature and outlet temperature of primary side

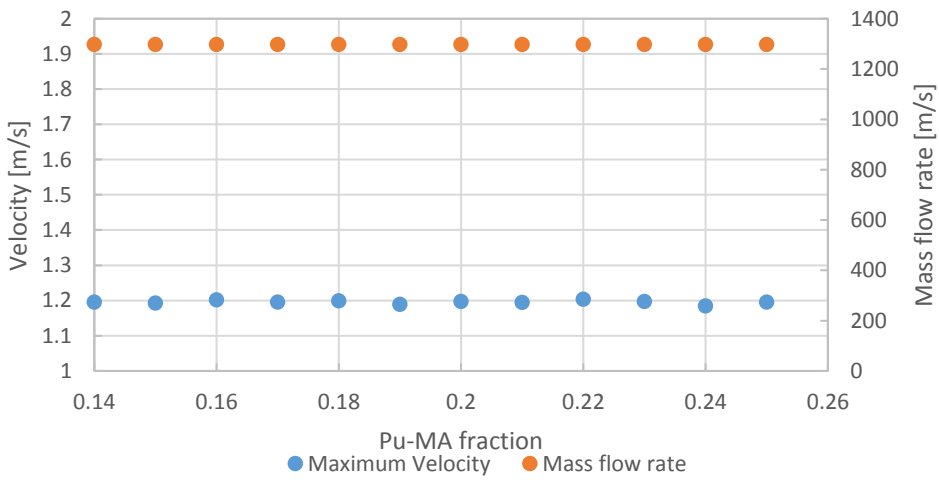

Figure 5-7 Influence of Pu-MA fraction on the whole core mass flow rate and maximum velocity

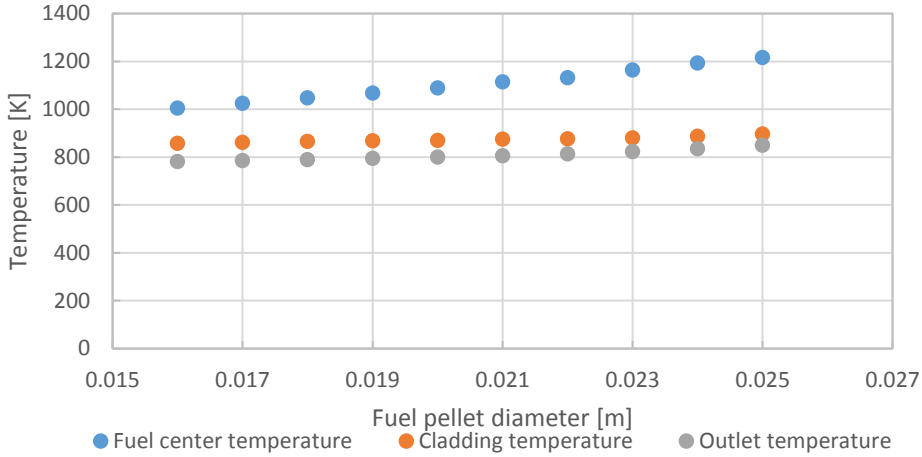

Figure 5-8 Influence of fuel pellet diameter on the fuel center temperature, cladding temperature and outlet temperature of primary side

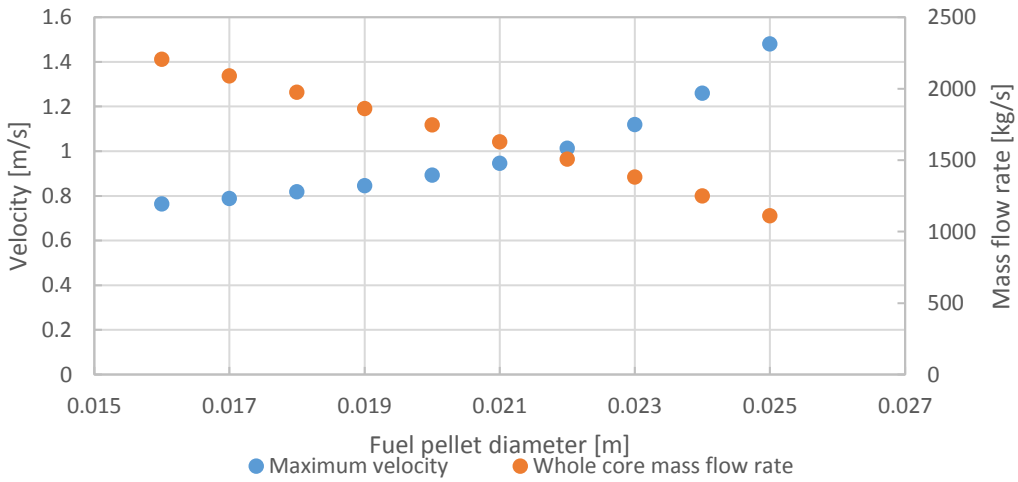

Figure 5-9 Influence of fuel pellet diameter on the whole core mass flow rate and maximum velocity

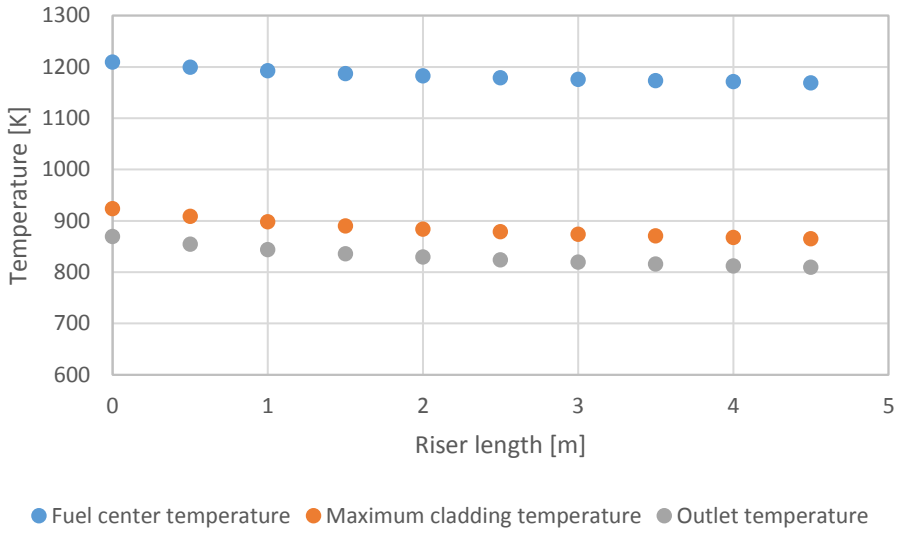

Figure 5-10 Influence of length of riser on the fuel center temperature, cladding temperature and outlet temperature of primary side

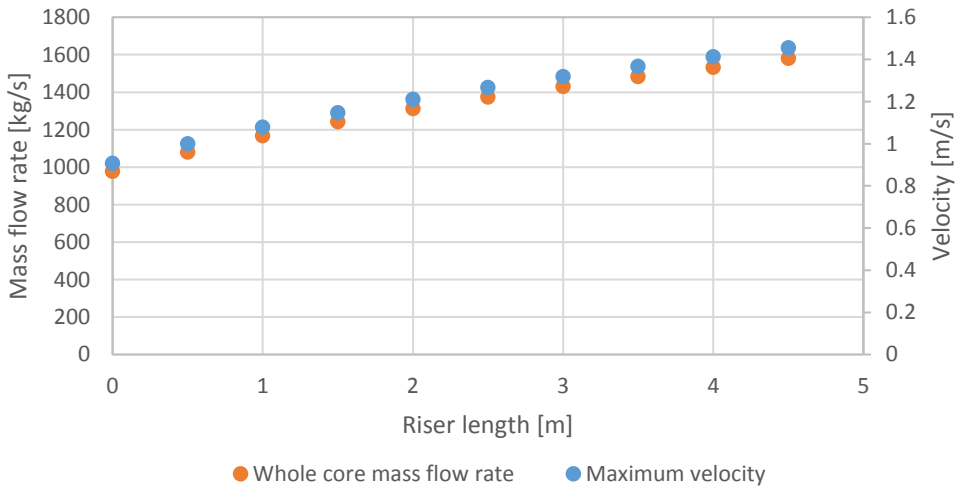

Figure 5-11 Influence of length of riser on the whole core mass flow rate and maximum velocity

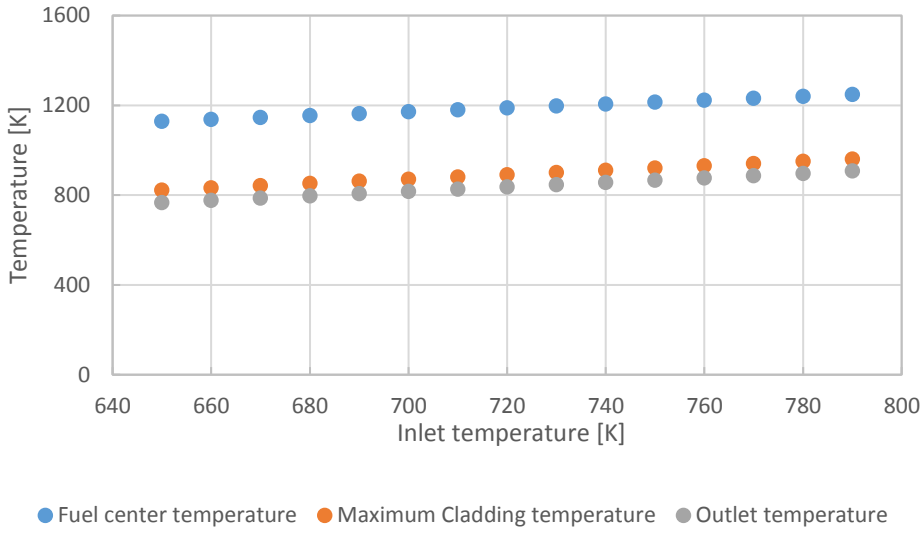

Figure 5-12 Influence of inlet temperature on the fuel center temperature, cladding temperature and outlet temperature of primary side

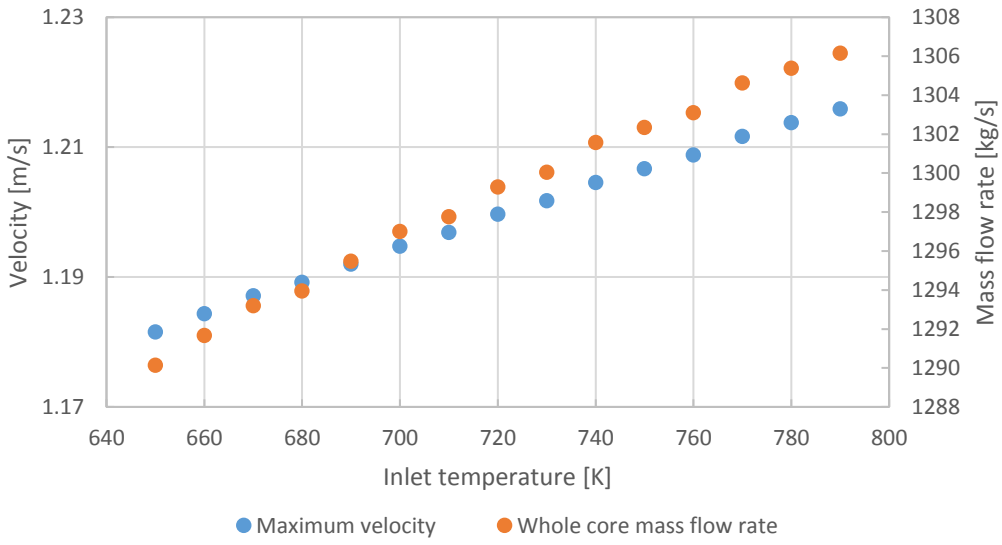

Figure 5-13 Influence of inlet temperature on the whole core mass flow rate and maximum velocity

6. Optimization Implementation and Results

Totally ten runs, each with 100 generations, are implemented in the Genetic Algorithm with “valuable phenotype” archival rule and the Genetic Algorithm without “Valuable phenotype” archival rule. In these implementations, the population size is 32, the mutation probability is 0.2, and the crossover probability is 0.8. The results are shown in table 6-1. It can be observed that the Genetic Algorithm with “valuable phenotype” archival rule has the overwhelming performance than the Genetic Algorithm without “valuable phenotype” archival rule. It is especially interesting to find that the run3, run6, run8 and run10 of the Genetic Algorithm without “valuable phenotype” archival rule has not dig out any dominant solution. For those implementations, the overall accomplishment of the Obj1 is relatively low.

To look insight of these implementations, the performance of the archived members in each generation of run6 is taken as an example and it is presented in the figure 6-1. At the beginning, the number of individuals accomplished Obj2 is much higher than Obj1, which means the Obj2 is much easier than Obj1 to be accomplished. Only after a few generations, the Obj2, Obj3 and Obj4 have been accomplished in most or all of the members archived. However, the archived members accomplished Obj1 never increase. Evidently, the searching direction has been biased to the neighbor local optimum that falls into “local optimum trap”. Another example shown in figure 6-2 demonstrate the same fact in run1 though totally 5 non-dominant solutions that dominate the chosen solution are found. In the

archived members, the Obj1 also suffers the insufficient accomplishment in the first 25 generations until when the first dominant solution is found. The figure 6-3 shows the results of the performance of the Genetic Algorithm with “valuable phenotype” archival rule in generation series. It can be found that the Obj1 is detected to be the hardest objective at the very beginning. Then the members with the “valuable phenotype” obtains the priority to enter the archive so that more offspring with the “valuable phenotype” will be produced. Thus, the valuable individuals are archived increasingly. The first dominant solution is found expeditiously in generation 9. From the results observed now, it suggests that the GA with “valuable phenotype” archival rule has better efficiency to find the dominant solutions. The figures 6-4 to 6-7 present the non-dominant phenotypic and genotypic population distribution in the overall 10 runs. It can be observed that the GA with “valuable phenotype” archival rule can find more dominant solutions and maintains better diversity as well. Thus, the designer will have more choices when zooms in the interest Pseudo-local-optimum.

Table 6-1 Ten implementations results of the Genetic Algorithm with "valuable phenotype" archival rule and without "valuable phenotype" archival rule

The archive without the rule of "valuable phenotype"						
	Obj1	Obj2	Obj3	Obj4	Dominated solutions number	Overall dominated solutions number in 10 runs
Run1	0.13	0.28	0.25	0.34	5	14
Run2	0.15	0.27	0.25	0.33	2	
Run3	0.01	0.38	0.25	0.36	0	
Run4	0.18	0.25	0.27	0.28	7	
Run5	0.18	0.24	0.26	0.32	7	
Run6	0.02	0.36	0.29	0.33	0	
Run7	0.19	0.25	0.26	0.30	2	
Run8	0.01	0.36	0.30	0.33	0	
Run9	0.19	0.23	0.26	0.32	6	
Run10	0.05	0.32	0.28	0.35	0	
The archive with the rule of "valuable phenotype"						
	Obj1	Obj2	Obj3	Obj4	Dominated solutions number	Overall dominated solutions number in 10 runs
Run1	0.20	0.24	0.25	0.31	23	54
Run2	0.22	0.23	0.25	0.30	10	
Run3	0.19	0.24	0.27	0.30	8	
Run4	0.18	0.25	0.25	0.32	15	
Run5	0.17	0.26	0.25	0.32	8	
Run6	0.13	0.31	0.21	0.35	8	
Run7	0.17	0.27	0.26	0.30	20	
Run8	0.18	0.27	0.25	0.30	10	
Run9	0.20	0.23	0.26	0.31	14	
Run10	0.16	0.26	0.26	0.32	8	

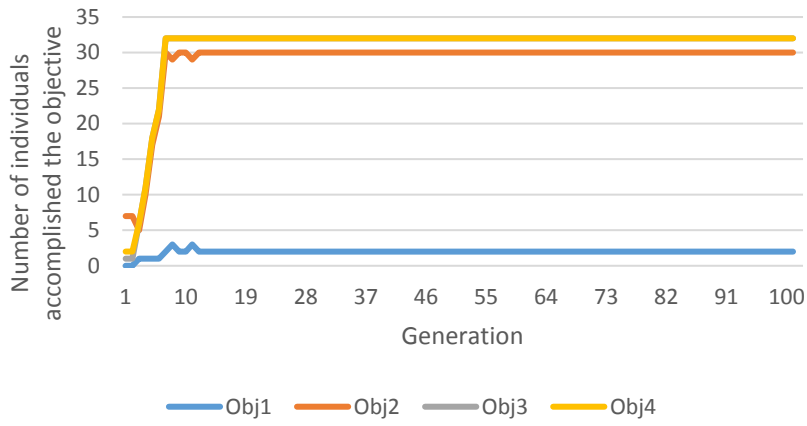

Figure 6-1 The number of individuals accomplished the objectives in the run6 of the archive without the rule of "valuable phenotype"

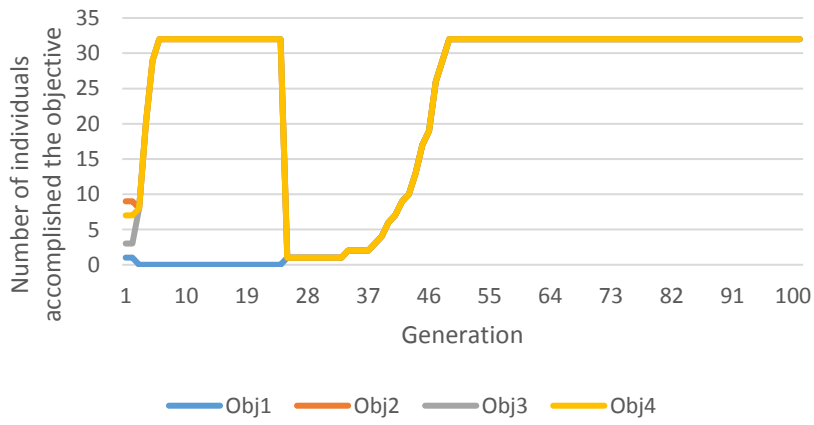

Figure 6-2 The number of individuals accomplished the objectives in the run1 of the archive without the rule of "valuable phenotype"

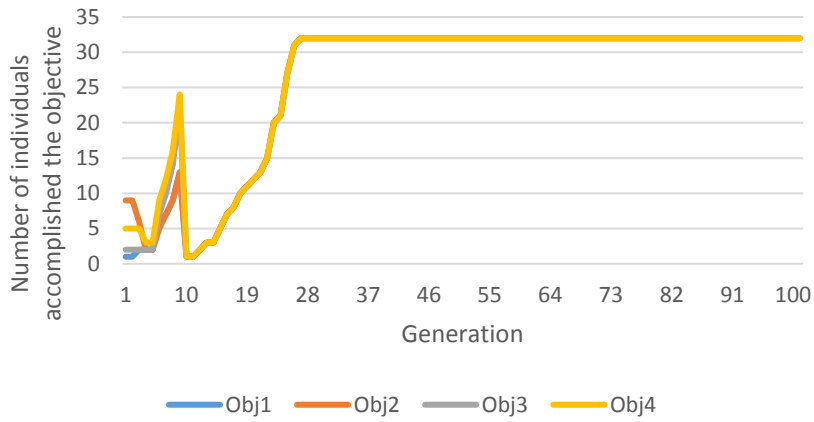

Figure 6-3 The number of individuals accomplished the objectives in the run1 of the archive with the rule of "valuable phenotype"

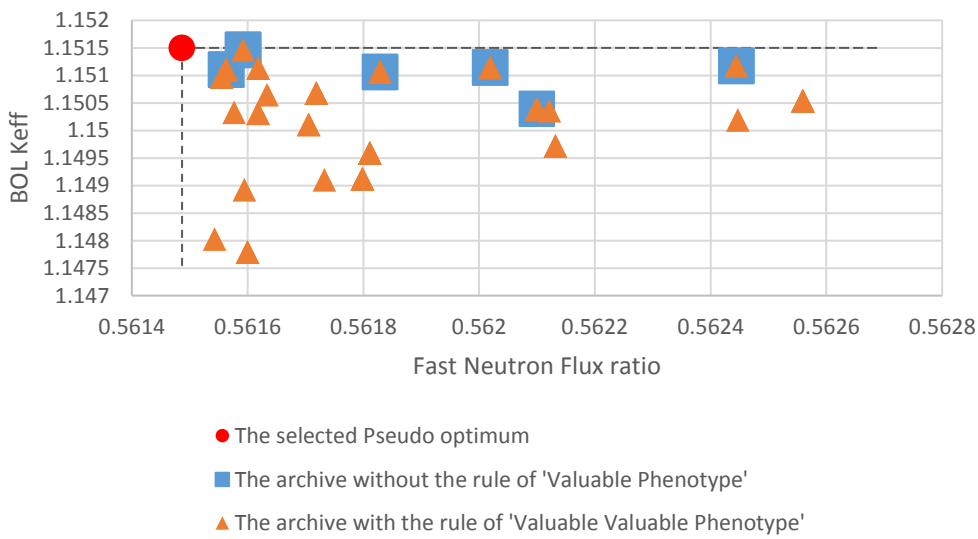

Figure 6-4 Phenotypic population distribution of BOL Keff and fast neutron flux ratio

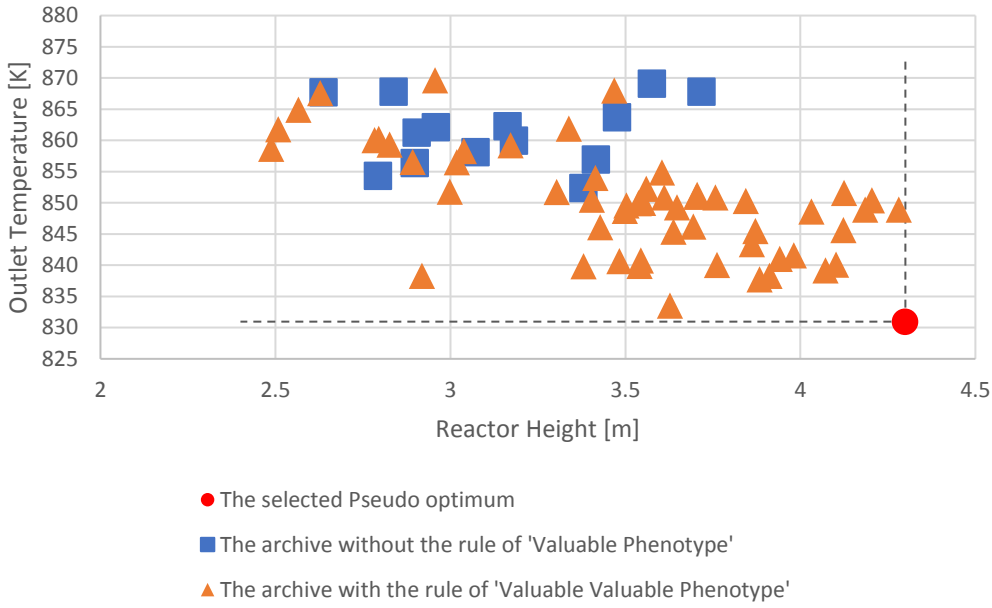

Figure 6-5 Phenotypic population distribution of outlet temperature and reactor height

Figure 6-6 Genotypic population distribution of Pu-MA fraction and fuel pellet diameter

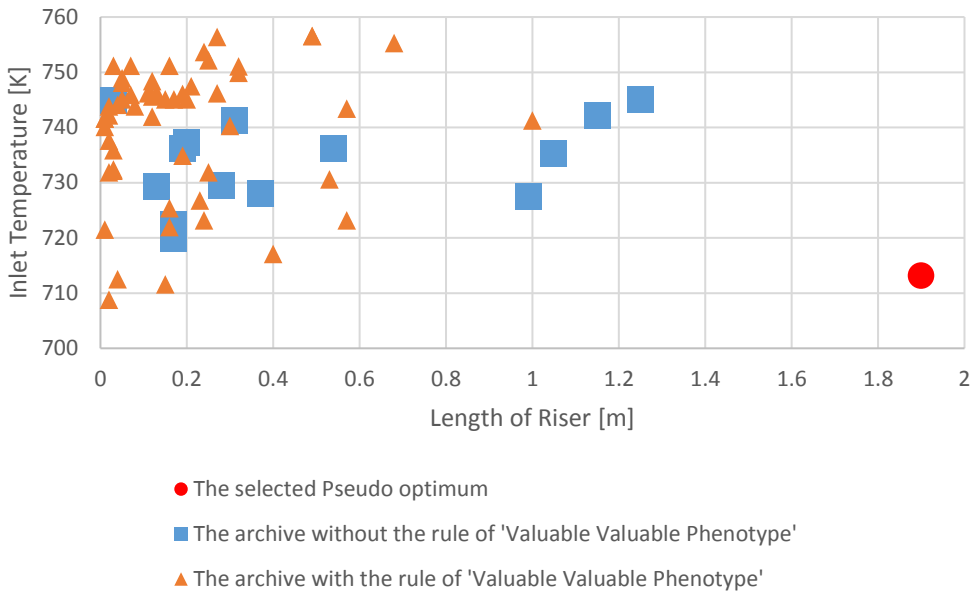

Figure 6-7 Genotypic population distribution of length of riser and inlet temperature

7. Conclusion

The LOGA is developed in this work and implemented in the BORIS design optimization problem. The foregoing results present that the Genetic Algorithm with archival rule of "valuable phenotype" is predominant than the Genetic Algorithm without archival rule of "valuable phenotype" in finding a higher tier of solutions in this reactor core design problem. By using the archival rule of "valuable phenotype", the searching can be guided to appreciate the accomplishment of the tough objective and keep the archive with the balanced population; eventually, reveal more solutions. The evolution process demonstrates the high efficiency and robustness of the LOGA.

REFERENCES

Ahn, Y., Jun, S., Kim, M., Kuk, S., Baik, S., Ik, J., & Eun, J. A. E. (2015). REVIEW OF SUPERCRITICAL CO 2 POWER CYCLE TECHNOLOGY AND CURRENT STATUS OF RESEARCH AND DEVELOPMENT. *Nuclear Engineering and Technology*, *47*(6), 647–661. https://doi.org/10.1016/j.net.2015.06.009

Alkhayri, W. R. (2016). A New Selection Operator - CSM in Genetic Algorithms for Solving the TSP, *7*(10), 62–66.

Allen, T. R., & Crawford, D. C. (2007). Lead-Cooled Fast Reactor Systems and the Fuels and Materials Challenges. *Science and Technology of Nuclear Installations*, *2007*, 1–11. https://doi.org/10.1155/2007/97486

Buongiomo, J. (2001). Conceptual Design of a Lead-Bismuth Cooled Fast Reactor with In-Vessel Direct-Contact Steam Generation Conceptual Design of a Lead-Bismuth Cooled Fast Reactor with In- Vessel Direct-Contact Steam Generation, (1996).

Buongiorno, J., Davis, C., Herring, S., Macdonald, P., Loewen, E., Smolik, G., … Todreas, N. (2001). Design of an Actinide Burning, Lead or Lead-Bismuth Cooled Reactor that Produces Low Cost Electricity Cooled Reactor that Produces Low Cost Electricity. *Ineel/Ext-01-01376*, (October 2001). https://doi.org/10.2172/773994

Chen, X., & Suh, K. Y. (2016). Development and Validation of a Momentum Integral Numerical Analysis Code for Liquid Metal Fast Reactor. In *Transactions of the Korean Nuclear Society Spring Meeting*. Jeju.

Cheng, X., & Tak, N. Il. (2006). Investigation on turbulent heat transfer to lead-bismuth eutectic flows in circular tubes for nuclear applications. *Nuclear Engineering and Design*, *236*(4), 385–393. https://doi.org/10.1016/j.nucengdes.2005.09.006

Cheon, J. S., Lee, C. B., Lee, B. O., Raison, J. P., Mizuno, T., Delage, F., & Carmack, J. (2009). Sodium fast reactor evaluation: Core materials. *Journal of Nuclear Materials*, *392*(2), 324–330. https://doi.org/10.1016/j.jnucmat.2009.03.021

Choi, D. H., & Oh, S. Y. (2000). A new mutation rule for evolutionary programming motivated from backpropagation learning. *IEEE Transactions on Evolutionary Computation*, *4*(2), 188–190. https://doi.org/10.1109/4235.850659

Choi, H., & Downar, T. J. (1999). A Liquid-Metal Reactor for Burning Minor Actinides of Spent Light Water Reactor Fuel — I : Neutronics Design Study, 1–22.

D. Dasgupta, Z. M. (1997). *Evolutionary Algorithms in Engineering Applications*.

Deb, K., Pratap, A., Agarwal, S., & Meyarivan, T. (2002). A fast and elitist multiobjective genetic algorithm: NSGA-II. *IEEE Transactions on Evolutionary Computation*, *6*(2), 182–197. https://doi.org/10.1109/4235.996017

Deep, K., & Thakur, M. (2007). A new crossover operator for real coded genetic algorithms, *188*, 895–911. https://doi.org/10.1016/j.amc.2006.10.047

Edenius, M., Ekberg, K., Forssén, B., & Knott, D. (1995). CASMO-4, A Fuel

Assembly Burnup Program, User's Manual. *Studsvik0SOA-9501, Studsvik of America*.

FRAAS, A., & OZISIK, M. (1965). Heat exchanger design(Book on fluid flow and heat transfer for designing, selecting, testing and installing various heat exchangers). *NEW YORK, JOHN WILEY AND SONS, INC., 1965.*

GIF, A. Technology Roadmap Update for Generation IV Nuclear Energy Systems. *Technical Report*, 2014.

Goldberg, D. E. (1989). *Genetic Algorithms in Search, Optimization, and Machine Learning*. *Addison Wesley* (Vol. Addison-We). https://doi.org/10.1007/s10589-009-9261-6

H Nippert. (1929). *Über den Strömungsverlust in gekrümmten Kanälen*.

Haupt, R. L., & Haupt, S. E. (2000). Optimum Population Size and Mutation Rate for a Simple Real Genetic Algorithm that Optimizes Array Factors. *Applied Computational Electromagnetics Society Newsletter*, *15*(2), 94–102. https://doi.org/10.1109/APS.2000.875398

Holland, J. H. (1975). *Adaptation in Natural and Artificial Systems*. *Ann Arbor MI University of Michigan Press* (Vol. Ann Arbor). https://doi.org/10.1137/1018105

Hutter, M. (2002). Fitness uniform selection to preserve genetic diversity. In *Proceedings of the 2002 Congress on Evolutionary Computation, CEC 2002* (Vol. 1, pp. 783–788). https://doi.org/10.1109/CEC.2002.1007025

Hyun, J., Batta, A., Casamassima, V., Cheng, X., Joon, Y., Soon, I., … Puspitarini, D. (2011). Benchmarking of thermal hydraulic loop models for Lead-Alloy Cooled Advanced Nuclear Energy System (LACANES), phase-I : Isothermal

steady state forced convection. *Journal of Nuclear Materials*, *415*(3), 404–414. https://doi.org/10.1016/j.jnucmat.2011.04.043

Idelchik, I. (1953). Determination of the resistance coefficients during discharge through orifices. *Gidrotekh Stroit*.

Jayalal, M. L., Murty, S. A. V. S., & Baba, M. S. (2014). A Survey of Genetic Algorithm Applications in Nuclear Fuel Management, *4*(1), 45–62.

Jong, K. A. De. (2005). Evolutionary Computation. *Vital*, *2*(3), 272. https://doi.org/10.1038/vital306-2a

Kaya, M. (2011). The effects of two new crossover operators on genetic algorithm performance. *Applied Soft Computing Journal*, *11*(1), 881–890. https://doi.org/10.1016/j.asoc.2010.01.008

Kumar, A., & Tsvetkov, P. V. (2015a). A new approach to nuclear reactor design optimization using genetic algorithms and regression analysis. *Annals of Nuclear Energy*, *85*, 27–35. https://doi.org/10.1016/j.anucene.2015.04.028

Kumar, A., & Tsvetkov, P. V. (2015b). Optimization of U – Th fuel in heavy water moderated thermal breeder reactors using multivariate regression analysis and genetic algorithms. *Annals of Nuclear Energy*, *85*, 885–892. https://doi.org/10.1016/j.anucene.2015.07.006

Laporte, G. (1992). The traveling salesman problem: An overview of exact and approximate algorithms. *European Journal of Operational Research*, *59*(2), 231–247. https://doi.org/10.1016/0377-2217(92)90138-Y

Leibowitz, L., & Blomquist, R. A. (1988). Thermal conductivity and thermal expansion of stainless steels D9 and HT9. *International Journal of Thermophysics*,

9(5), 873–883. https://doi.org/10.1007/BF00503252

Matsui, K. (1999). New selection method to improve the population diversity in genetic algorithms. *IEEE SMC'99 Conference Proceedings. 1999 IEEE International Conference on Systems, Man, and Cybernetics (Cat. No.99CH37028)*, *1*, 625–630. https://doi.org/10.1109/ICSMC.1999.814164

Massey, B. S., & Ward-Smith, J. (1998). *Mechanics of fluids* (Vol. 1). CRC Press.

Muta, H., Kurosaki, K., Uno, M., & Yamanaka, S. (2008). Thermal and mechanical properties of uranium nitride prepared by SPS technique. *Journal of Materials Science*, *43*(19), 6429–6434. https://doi.org/10.1007/s10853-008-2731-x

OKUMURA, K., MORI, T., NAKAGAWA, M., & KANEKO, K. (2000). Validation of a Continuous-Energy Monte Carlo Burn-up Code MVP-BURN and Its Application to Analysis of Post Irradiation Experiment. *Journal of Nuclear Science and Technology*, *37*(2), 128–138. https://doi.org/10.1080/18811248.2000.9714876

Pacio, J. (2015). Eutectic Alloy and Lead Properties , Materials Compatibility , Thermal- hydraulics and Technologies 2015 Edition H andbook on Lead-bismuth, 647–730.

Pahl, R. G., Lahm, C. E., & Hayes, S. L. (1993). Performance of HT9 clad metallic fuel at high temperature. *Journal of Nuclear Materials*, *204*(C), 141–147. https://doi.org/10.1016/0022-3115(93)90210-P

Pahl, R. G., Porter, D. L., Lahm, C. E., & Hofman, G. L. (1990). Experimental studies of U-Pu-Zr fast reactor fuel pins in the experimental breeder reactor-ll. *Metallurgical Transactions A*, *21*(7), 1863–1870. https://doi.org/10.1007/BF02647233

Parks, G. T. (1996). Multiobjective Pressurized Water Reactor Reload Core Design by Nondominated Genetic Algorithm Search, *187*, 178–187.

Poon, P. W., & Carter, J. N. (1995). Genetic algorithm crossover operators for ordering applications. *Computers and Operations Research*, *22*(1), 135–147. https://doi.org/10.1016/0305-0548(93)E0024-N

Qualls, A. L., Betzler, B. R., Brown, N. R., Carbajo, J. J., Greenwood, M. S., Hale, R., … Worrall, A. (2017). Preconceptual design of a fluoride high temperature salt-cooled engineering demonstration reactor : Motivation and overview q. *Annals of Nuclear Energy*, *107*, 144–155. https://doi.org/10.1016/j.anucene.2016.11.021

Schikorr, M., Bubelis, E., Mansani, L., & Litfin, K. (2010). Proposal for pressure drop prediction for a fuel bundle with grid spacers using Rehme pressure drop correlations. *Nuclear Engineering and Design*, *240*(7), 1830–1842. https://doi.org/10.1016/j.nucengdes.2010.03.039

Shim, H.-J., Han, B.-S., Jung, J.-S., Park, H.-J., & Kim, C.-H. (2012). Mccard: Monte Carlo Code for Advanced Reactor Design and Analysis. *Nuclear Engineering and Technology*, *44*(2), 161–176. https://doi.org/10.5516/NET.01.2012.503

Smith, M. A., Kim, S. J., Bodnar, Y. D., & Wade, D. C. (2005). SSTAR Lead-Cooled, Small Modular Fast Reactor with Nitride Fuel. *... on Advanced Reactors …*. Retrieved from https://oecd-nea.org/science/meetings/ARWIF2004/2.03.pdf%5Cnpapers3://publication/uuid/9BBDFBA0-8CED-4F3E-8EBD-EF33A5EDE27A

Sobolev, V., Malambu, E., & Abderrahim, H. A. (2009). Design of a fuel element for a lead-cooled fast reactor. *Journal of Nuclear Materials*, *385*(2), 392–

399. https://doi.org/10.1016/j.jnucmat.2008.12.027

Son, H. M., & Suh, K. Y. (2011). Evolutionary design of reactor vessel assembly for liquid metal cooled battery. *Progress in Nuclear Energy*, *53*(7), 825–830. https://doi.org/10.1016/j.pnucene.2011.05.026

Son, H. M., & Suh, K. Y. (2014). Automated scoping methodology for liquid metal natural circulation small reactor. *Nuclear Engineering and Design*, *274*, 129–145. https://doi.org/10.1016/j.nucengdes.2014.04.020

Srinivas, N., & Deb, K. (1994). Multiobjective Optimization Using Nondominated Sorting in Genetic Algorithms 1 Introduction. *Evolutionary Computation*, *2*(3), 221–248.

Stamm'ler, R. (1998). HELIOS methods. *Studsvik Scandpower*.

Tak, T., Lee, D., & Kim, T. K. (2013). Design of ultralong-cycle fast reactor employing breed-and-burn strategy. *Nuclear Technology*, *183*(3).

Todreas, N. E. (2001). Minor actinide burning in dedicated lead-bismuth cooled fast reactors *. In *9th Int. Conf. of Nucl* (pp. 8–12).

Toshinsky, V. G., Sekimoto, H., & Toshinsky, G. I. (2000). Method to improve multiobjective genetic algorithm optimization of a self-fuel-providing LMFBR by niche induction among nondominated solutions. *Annals of Nuclear Energy*, *27*(5), 397–410. https://doi.org/10.1016/S0306-4549(99)00065-1

Wu, S. J., & Chow, P. T. (1995). Steady-state genetic algorithms for discrete optimization of trusses. *Computers and Structures*, *56*(6), 979–991. https://doi.org/10.1016/0045-7949(94)00551-D

Zhang, M., Gao, X., & Lou, W. (2007). A new crossover operator in genetic

programming for object classification. *IEEE Transactions on Systems, Man, and Cybernetics, Part B: Cybernetics*, *37*(5), 1332–1343. https://doi.org/10.1109/TSMCB.2007.902043

Zhang, Q., Sun, J., & Tsang, E. (2005). An evolutionary algorithm with guided mutation for the maximum clique problem. *IEEE Transactions on Evolutionary Computation*, *9*(2), 192–200. https://doi.org/10.1109/TEVC.2004.840835

Zhao, J., Tso, C. P., & Tseng, K. J. (2011). SCWR single channel stability analysis using a response matrix method. *Nuclear Engineering and Design*, *241*(7), 2528–2535. https://doi.org/10.1016/j.nucengdes.2011.04.026